

STANDARD MODEL THEORY

W. HOLLIK

Theoretical Physics Division, CERN
CH-1211 Geneva 23, Switzerland

and

Institut für Theoretische Physik, Universität Karlsruhe
D-76128 Karlsruhe, Germany

Abstract

In this conference report a summary is given on the theoretical work that has contributed to provide accurate theoretical predictions for testing the standard model in present and future experiments. Precision calculations for the vector boson masses, for the Z resonance, W pair production, and for the $g-2$ of the muon are reviewed and the theoretical situation for the Higgs sector is summarized. The status of the standard model is discussed in the light of the recent high and low energy data. New Physics beyond the standard model is briefly addressed as well, with special emphasis on the minimal supersymmetric standard model.

Plenary talk at the
XXIX International Conference on High Energy Physics
Vancouver, Canada, 23 - 29 July 1998

STANDARD MODEL THEORY

W. HOLLIK

Theoretical Physics Division, CERN, CH-1211 Geneva 23, Switzerland

and

Institut für Theoretische Physik, Universität Karlsruhe, D-76128 Karlsruhe, Germany

E-mail: Wolfgang.Hollik@physik.uni-karlsruhe.de

In this conference report a summary is given on the theoretical work that has contributed to provide accurate theoretical predictions for testing the standard model in present and future experiments. Precision calculations for the vector boson masses, for the Z resonance, W pair production, and for the $g - 2$ of the muon are reviewed and the theoretical situation for the Higgs sector is summarized. The status of the standard model is discussed in the light of the recent high and low energy data. New Physics beyond the standard model is briefly addressed as well, with special emphasis on the minimal supersymmetric standard model.

1 Introduction

The e^+e^- colliders LEP and the SLC, in operation since summer 1989, have collected an enormous amount of electroweak precision data on Z and W bosons^{1,2}. The W boson properties have in parallel been determined at the $p\bar{p}$ collider Tevatron with a constant increase in accuracy^{3,2}; after the discovery of the top quark there⁴, its mass has been measured⁵ with a precision of better than 3%, to 173.8 ± 5.0 GeV. The ongoing experiments at LEP 2 and the near-future Tevatron upgrade will also, in the coming years, support us with further increases in precision, in particular on the mass of the W and the top, and the SLC might continue to improve the impressive accuracy already obtained in the electroweak mixing angle. This stimulating experimental program together with the theoretical activities to provide accurate predictions from the standard model have formed the era of electroweak precision tests and will keep it alive also in the next years.

The standard theory of the electroweak interaction is a gauge-invariant quantum field theory with the symmetry group $SU(2) \times U(1)$ spontaneously broken by the Higgs mechanism. The possibility to perform perturbative calculations for observable quantities in terms of a few input parameters is substantially based on the renormalizability of this class of theories⁶. A certain set of input parameters has to be taken from experiment. In the electroweak standard model essentially three free parameters are required to describe the gauge bosons γ , W^\pm , Z , and their interactions with the fermions. For a comparison between theory and experiment, hence, three independent experimental input data are required. The most natural choice consists of the electromagnetic fine structure constant α , the muon decay constant (Fermi constant) G_μ , and the mass of the Z boson, which has meanwhile been measured with the same accuracy as the Fermi constant^{1,2}. Other measurable quantities are predicted in terms of the input data. Each additional pre-

cision experiment, which allows the detection of small deviations from the lowest-order predictions, can be considered a test of the electroweak theory at the quantum level. In the Feynman graph expansion of the scattering amplitude for a given process the higher-order terms show up as diagrams containing closed loops. The renormalizability of the standard model ensures that it retains its predictive power also in higher orders. The higher-order terms are the quantum effects of the electroweak theory. They are complicated in their concrete form, but they are finally the consequence of the basic Lagrangian with a simple structure. The quantum corrections (or “radiative corrections”) contain the self-coupling of the vector bosons as well as their interactions with the Higgs field and the top quark, and provide the theoretical basis for electroweak precision tests. Assuming the validity of the standard model, the presence of the top quark and the Higgs boson in the loop contributions to electroweak observables allows an indirect probe of their mass ranges from comparison with precision data.

The generation of high-precision experiments hence imposes stringent tests on the standard model. A primordial step strengthening our confidence in the standard model has been the discovery of the top quark at the Tevatron⁴, at a mass that agrees with the mass range obtained indirectly, through the radiative corrections. Moreover, with the top mass as an additional precise experimental data point one can now fully exploit the virtual sensitivity to the Higgs mass.

The experimental sensitivity in the electroweak observables, at the level of the quantum effects, requires the highest standards on the theoretical side as well. A sizeable amount of work has contributed, over the recent years, to a steadily rising improvement of the standard model predictions, pinning down the theoretical uncertainties to the level required for the current interpretation of the precision data. The availability of both highly accurate measurements and theoretical predictions, at the

level of 0.1% precision and better, provides tests of the quantum structure of the standard model, thereby probing its still untested scalar sector, and simultaneously accesses alternative scenarios such as the supersymmetric extension of the standard model.

The lack of direct signals from new physics beyond the standard model makes the high-precision experiments a unique tool also in the search for indirect effects: through possible deviations of the experimental results from the theoretical predictions of the minimal standard model. Since such deviations are expected to be small, it is decisive to have the standard loop effects in the precision observables under control.

This review contains a discussion of the theoretical developments for testing the electroweak theory, the status of the standard model in view of the most recent high and low energy data, and the implications for the Higgs boson. New Physics is briefly included, with main emphasis on the minimal supersymmetric standard model.

2 Status of precision calculations

2.1 Basic ingredients in radiative corrections

The possibility of performing precision tests is based on the formulation of the standard model as a renormalizable quantum field theory preserving its predictive power beyond tree-level calculations. With the experimental accuracy being sensitive to the loop-induced quantum effects, also the Higgs sector of the standard model is being probed. The higher-order terms induce the sensitivity of electroweak observables to the top and Higgs mass m_t, M_H and to the strong coupling constant α_s .

The calculation of electroweak observables in higher orders requires the concept of renormalization to get rid of the divergences in the Feynman integral evaluation and to define the physical input parameters. In QED and in the electroweak theory the classical Thomson scattering and the particle masses set natural scales where the parameters $e = \sqrt{4\pi\alpha}$ and the electron, muon, ... masses can be defined. In the electroweak standard model a distinguished set for parameter renormalization is given in terms of e, M_Z, M_W, M_H, m_f with the masses of the corresponding particles. The finite parts of the counter terms are fixed by the renormalization conditions that the propagators have poles at their physical masses, and e becomes the $ee\gamma$ coupling constant in the Thomson limit of Compton scattering. This electroweak on-shell scheme, the extension of the familiar QED renormalization, has been used in many practical applications⁷⁻¹⁷. The mass of the Higgs boson, as long as it is experimentally unknown, is treated as a free input parameter. In

practical calculations, the W mass is replaced by G_μ as an input parameter by using relation (18).

Instead of the set e, M_W, M_Z as basic free parameters other renormalization schemes make use of α, G_μ, M_Z ¹⁸ or perform the loop calculations in the \overline{MS} scheme¹⁹⁻²². Other schemes applied in the past utilize the parameters $\alpha, G_\mu, \sin^2\theta_W$, with the mixing angle deduced from neutrino-electron scattering²³, or the concept of effective running couplings^{24,25}.

Before predictions can be made from the theory, a set of independent parameters has to be taken from experiment. For practical calculations the physical input quantities $\alpha, G_\mu, M_Z, m_f, M_H, \alpha_s$ are commonly used to fix the free parameters of the standard model. Differences between various schemes are formally of higher order than the one under consideration. The study of the scheme dependence of the perturbative results, after improvement by resummation of the leading terms, allows us to estimate the missing higher-order contributions (see e.g.²⁶ for a comprehensive study).

Related to charge and mass renormalization, there occur two sizeable effects in the electroweak loops that deserve a special discussion:

(i) *Charge renormalization and light fermion contribution:*

Charge renormalization introduces the concept of electric charge for real photons ($q^2 = 0$) to be used for the calculation of observables at the electroweak scale set by M_Z . Hence the difference

$$\text{Re } \hat{\Pi}^\gamma(M_Z^2) = \text{Re } \Pi^\gamma(M_Z^2) - \Pi^\gamma(0) \quad (1)$$

of the photon vacuum polarization is a basic entry in the predictions for electroweak precision observables. The purely fermionic contributions correspond to standard QED and do not depend on the details of the electroweak theory. They are conveniently split into a leptonic and a hadronic contribution

$$\text{Re } \hat{\Pi}^\gamma(M_Z^2)_{\text{ferm}} = \text{Re } \hat{\Pi}_{\text{lept}}^\gamma(M_Z^2) + \text{Re } \hat{\Pi}_{\text{had}}^\gamma(M_Z^2), \quad (2)$$

where the top quark is not included in the hadronic part (5 light flavours); it yields a small non-logarithmic contribution

$$\hat{\Pi}_{\text{top}}^\gamma(M_Z^2) \simeq \frac{\alpha}{\pi} Q_t^2 \frac{M_Z^2}{5 m_t^2} \simeq 0.57 \cdot 10^{-4}. \quad (3)$$

The quantity

$$\begin{aligned} \Delta\alpha &= \Delta\alpha_{\text{lept}} + \Delta\alpha_{\text{had}} \\ &= -\text{Re } \hat{\Pi}_{\text{lept}}^\gamma(M_Z^2) - \text{Re } \hat{\Pi}_{\text{had}}^\gamma(M_Z^2) \end{aligned} \quad (4)$$

corresponds to a QED-induced shift in the electromagnetic fine structure constant

$$\alpha \rightarrow \alpha(1 + \Delta\alpha), \quad (5)$$

which can be resummed according to the renormalization group accommodating all the leading logarithms of the type $\alpha^n \log^n(M_Z/m_f)$. The result can be interpreted as an effective fine structure constant at the Z mass scale:

$$\alpha(M_Z^2) = \frac{\alpha}{1 - \Delta\alpha}. \quad (6)$$

It corresponds to a resummation of the iterated 1-loop vacuum polarization from the light fermions to all orders.

$\Delta\alpha$ is an input of crucial importance because of its universality and of its remarkable size of $\sim 6\%$. The leptonic content can be directly evaluated in terms of the known lepton masses, yielding at one loop order:

$$\Delta\alpha_{\text{lept}} = \sum_{\ell=e,\mu,\tau} \frac{\alpha}{3\pi} \left(\log \frac{M_Z^2}{m_\ell^2} - \frac{5}{3} \right) + O\left(\frac{m_\ell^2}{M_Z^2}\right). \quad (7)$$

The 2-loop correction has been known already for a long time²⁷, and also the 3-loop contribution is now available²⁸, yielding altogether

$$\begin{aligned} \Delta\alpha_{\text{lept}} &= 314.97687 \cdot 10^{-4} = \\ &[314.19007_{1\text{-loop}} + 0.77617_{2\text{-loop}} + 0.0106_{3\text{-loop}}] \cdot 10^{-4}. \end{aligned} \quad (8)$$

For the light hadronic part, perturbative QCD is not applicable and quark masses are not available as reasonable input parameters. Instead, the 5-flavour contribution to $\hat{\Pi}_{\text{had}}^\gamma$ can be derived from experimental data with the help of a dispersion relation

$$\Delta\alpha_{\text{had}} = -\frac{\alpha}{3\pi} M_Z^2 \text{Re} \int_{4m_\pi^2}^{\infty} ds' \frac{R^\gamma(s')}{s'(s' - M_Z^2 - i\varepsilon)} \quad (9)$$

with

$$R^\gamma(s) = \frac{\sigma(e^+e^- \rightarrow \gamma^* \rightarrow \text{hadrons})}{\sigma(e^+e^- \rightarrow \gamma^* \rightarrow \mu^+\mu^-)}$$

as an experimental input quantity in the problematic low energy range.

Integrating by means of the trapezoidal rule (averaging data in bins) over e^+e^- data for the energy range below 40 GeV and applying perturbative QCD for the high-energy region above, the expression (9) yields the value^{29,30}

$$\Delta\alpha_{\text{had}} = -0.0280 \pm 0.0007, \quad (10)$$

which agrees with another independent analysis³¹ with a different error treatment. Because of the lack of precision in the experimental data a large uncertainty is associated

with the value of $\Delta\alpha_{\text{had}}$, which propagates into the theoretical error of the predictions of electroweak precision observables. Including additional data from τ -decays³² yields about the same result with a slightly improved uncertainty. Recently other attempts have been made to increase the precision of $\Delta\alpha$ ^{33,35–37} by “theory-driven” analyses of the dispersion integral (9). The common basis is the application of perturbative QCD down to the energy scale given by the τ mass for the calculation of the quantity $R^\gamma(s)$ outside the resonances. Those calculations were made possible by the recent availability of the quark-mass-dependent $O(\alpha_s^2)$ QCD corrections³⁸ for the cross section down to close to the thresholds for b and c production. [A first step in this direction was done in³⁹ in the massless approximation.] In order to pin down the error, two different strategies are in use: the application of the method developed in³⁶ for minimizing the impact of data from less reliable regions, done in³³, and the rescaling of data in the open charm region of 3.7–5 GeV from PLUTO/DASP/MARKII, for the purpose of normalization to agree with perturbative QCD, done in³⁵. The results obtained for $\Delta\alpha_{\text{had}}$ are very similar:

$$\begin{aligned} &0.02763 \pm 0.0016 \quad \text{ref}^{33} \\ &0.02777 \pm 0.0017 \quad \text{ref}^{35} \end{aligned}$$

In³⁷ the \overline{MS} quantity $\hat{\alpha}(M_Z)$ has been derived with the help of an unsubtracted dispersion relation in the \overline{MS} -scheme, yielding a comparable error. The history of the determination of the hadronic vacuum polarization is visualized in Figure 1.

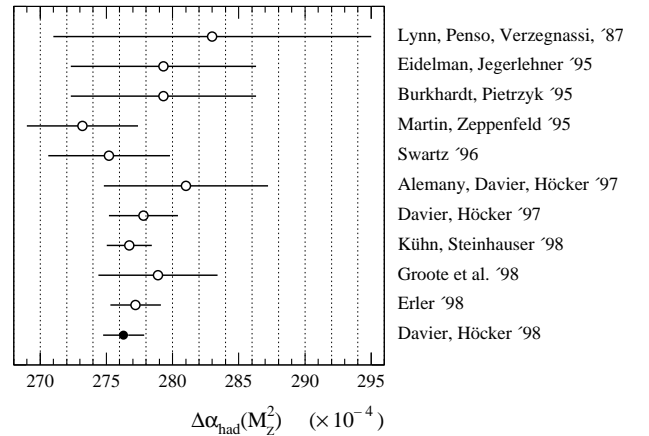


Figure 1: Various determinations of $\Delta\alpha_{\text{had}}$ (from ref³⁴).

The basic assumption in the theory-driven approach, the validity of perturbative QCD and quark-hadron duality, is supported by the following empirical observations:

– The strong coupling constant $\alpha_s(m_\tau)$ determined from hadronic τ decays shows good agreement with

$\alpha_s(M_Z)$ determined from Z -peak observables when the renormalization group evolution of α_s in perturbative QCD is imposed to run α_s from m_τ to the Z -mass scale.

– Non-perturbative contributions in $R^\gamma(s)$, parametrized in terms of condensates of quarks, gluons and of vacuum expectation values of higher-dimensional operators in the operator product expansion⁴⁰ can be probed by comparing spectral moments of $R_{\text{exp}}^\gamma(s)$ with the corresponding expressions involving the theoretical R^γ . It has been shown from fitting a set of moments that the non-perturbative contributions are negligibly small^{33,34}.

– Recent preliminary measurements of R^γ at BES at 2.6 and 3.3 GeV show values slightly lower than the previous data^{41,2}, better in alignment with the expectations from perturbative QCD.

Although the error in the QCD-based evaluation of $\Delta\alpha_{\text{had}}$ is considerably reduced, it should be kept in mind that the conservative estimate in Eq. (10) is independent of theoretical assumptions on QCD at lower energies and thus less sensitive to potential systematic effects not under consideration now⁴².

(ii) *Mixing angle renormalization and the ρ -parameter:*

The ρ -parameter, originally defined as the ratio of the neutral to the charged current strength in neutrino scattering⁴³, is unity in the standard model at the tree level, but gets a deviation $\Delta\rho$ from 1 by radiative corrections. The dominating universal part has its origin in the renormalization of the relation between the gauge boson masses and the electroweak mixing angle. This relation is modified in higher orders according to

$$\sin^2 \theta_W = 1 - \frac{M_W^2}{M_Z^2} + \frac{M_W^2}{M_Z^2} \Delta\rho + \dots \quad (11)$$

The main contribution to the universal ρ -parameter

$$\rho = \frac{1}{1 - \Delta\rho} \quad (12)$$

is from the (t, b) doublet⁴⁴, at the present level calculated as follows:

$$\Delta\rho = 3x_t \cdot [1 + x_t \rho^{(2)} + \delta\rho_{\text{QCD}}] \quad (13)$$

with

$$x_t = \frac{G_\mu m_t^2}{8\pi^2 \sqrt{2}}. \quad (14)$$

The electroweak 2-loop part^{45,46} is described by the function $\rho^{(2)}(M_H/m_t)$, and $\delta\rho_{\text{QCD}}$ is the QCD correction to the leading $G_\mu m_t^2$ term^{47,48}

$$\delta\rho_{\text{QCD}} = -\frac{\alpha_s(\mu)}{\pi} c_1 + \left(\frac{\alpha_s(\mu)}{\pi}\right)^2 c_2(\mu) \quad (15)$$

with

$$c_1 = \frac{2}{3} \left(\frac{\pi^2}{3} + 1 \right) = 2.8599$$

and the 3-loop coefficient⁴⁸ $c_2(\mu)$, which amounts to

$$c_2 = -14.59 \quad \text{for } \mu = m_t \text{ and 6 flavours}$$

with the on-shell top mass m_t . This reduces the scale dependence of ρ significantly and hence is an important entry to decrease the theoretical uncertainty of the standard model predictions for precision observables.

There is also a Higgs contribution to $\Delta\rho$, which, however, is not UV-finite by itself when derived from only the diagrams involving the physical Higgs boson. The M_H -dependence for large Higgs masses M_H is only logarithmic in 1-loop order⁴⁹; the 2-loop contribution⁵⁰ shows a dependence $\sim M_H^2$ for large values of the Higgs mass. In the limit $\sin^2 \theta_W \rightarrow 0$, $M_Z \rightarrow M_W$, where the $U(1)_Y$ is switched off, one finds $\Delta\rho_H = 0$. This is the consequence of the global $SU(2)_R$ symmetry of the Higgs Lagrangian (‘custodial symmetry’), which is broken by the $U(1)_Y$ group. Thus, $\Delta\rho_H$ is a measure of the $SU(2)_R$ breaking by the weak hypercharge.

2.2 Muon decay and the vector boson masses

The interdependence between the gauge boson masses is established through the accurately measured muon lifetime or, equivalently, the Fermi coupling constant G_μ . Originally, the μ -lifetime τ_μ has been calculated within the framework of the effective 4-point Fermi interaction. Beyond the well-known 1-loop QED corrections⁵¹, the 2-loop QED corrections in the Fermi model have been calculated quite recently⁵², yielding the expression (the error in the 2-loop term is from the hadronic uncertainty)

$$\frac{1}{\tau_\mu} = \frac{G_\mu^2 m_\mu^5}{192\pi^3} \left(1 - \frac{8m_e^2}{m_\mu^2} \right) \cdot \left[1 + 1.810 \frac{\alpha}{\pi} + (6.701 \pm 0.002) \left(\frac{\alpha}{\pi} \right)^2 \right]. \quad (16)$$

This formula is the defining equation for G_μ in terms of the experimental μ -lifetime. Owing to the presence of order-dependent QED corrections, the numerical value of the Fermi constant changes after the second-order term is included. Compared with the value given in the 1998 report of the Particle Data Group⁵³, the latest value is now smaller by $2 \cdot 10^{-10} \text{ GeV}^{-2}$, namely⁵²

$$G_\mu = (1.16637 \pm 0.00001) \cdot 10^{-5} \text{ GeV}^{-2}, \quad (17)$$

where also the error has been reduced by a factor of about 1/2.

In the standard model, G_μ can be calculated including quantum corrections in terms of the basic standard

model parameters, thereby separating off all diagrams that correspond to the QED corrections in the Fermi model. This yields the correlation between the masses M_W, M_Z of the vector bosons, expressed in terms of α and G_μ ; in 1-loop order it is given by⁹:

$$\frac{G_\mu}{\sqrt{2}} = \frac{\pi\alpha}{2s_W^2 M_W^2} [1 + \Delta r(\alpha, M_W, M_Z, M_H, m_t)]. \quad (18)$$

with $s_W^2 = 1 - M_W^2/M_Z^2$.

The decomposition

$$\Delta r = \Delta\alpha - \frac{c_W^2}{s_W^2} \Delta\rho^{(1)} + (\Delta r)_{\text{rem}} \quad (19)$$

separates the leading fermionic contributions $\Delta\alpha$ and $\Delta\rho$ (1-loop). All other terms are collected in the remainder part $(\Delta r)_{\text{rem}}$, the typical size of which is of order ~ 0.01 .

The presence of large terms in Δr requires the consideration of effects higher than 1-loop (see also the contribution by Kühn⁵⁴ to these proceedings). The modification of Eq. (18) according to

$$\begin{aligned} 1 + \Delta r &\rightarrow \frac{1}{(1 - \Delta\alpha) \cdot (1 + \frac{c_W^2}{s_W^2} \Delta\rho) - (\Delta r)_{\text{rem}}} \\ &\equiv \frac{1}{1 - \Delta r} \end{aligned} \quad (20)$$

accommodates the following higher-order terms (Δr in the denominator is an effective correction including higher orders):

(i) the leading log resummation⁵⁵ of $\Delta\alpha$: $1 + \Delta\alpha \rightarrow (1 - \Delta\alpha)^{-1}$;

(ii) the resummation of the leading m_t^2 contribution⁵⁶ in terms of $\Delta\rho$ in Eq. (13). Beyond the QCD higher-order contributions through the ρ -parameter, the complete $O(\alpha\alpha_s)$ corrections to the self energies are available^{57,58}. All these higher-order terms contribute with the same positive sign to Δr . Non-leading QCD corrections to Δr of the type

$$\Delta r_{(bt)} = 3x_t \left(\frac{\alpha_s}{\pi}\right)^2 \left(a_1 \frac{M_Z^2}{m_t^2} + a_2 \frac{M_Z^4}{m_t^4}\right)$$

are also available⁵⁹.

(iii) With the quantity $(\Delta r)_{\text{rem}}$ in the denominator, non-leading higher-order terms containing mass singularities of the type $\alpha^2 \log(M_Z/m_f)$ from light fermions are incorporated⁶⁰.

(iv) The subleading $G_\mu^2 m_t^2 M_Z^2$ contribution of the electroweak 2-loop order⁶¹ in an expansion in terms of the top mass. This subleading term turned out to be

sizeable, about as large as the formally leading term of $O(m_t^4)$ via the ρ -parameter. In view of the present and future experimental accuracy it constitutes a non-negligible shift in the W mass.

Meanwhile exact results have been derived for the Higgs-dependence of the fermionic 2-loop corrections in Δr ⁶², and comparisons were performed with those obtained via the top mass expansion⁶³. Differences in the values of M_W of several MeV (up to 8 MeV) are observed when M_H is varied over the range from 65 GeV to 1 TeV.

Figure 2 shows the Higgs-mass dependence of the two-loop corrections to Δr associated with the t/b doublet, with $\Delta\alpha$, and with the light fermion terms not in $\Delta\alpha$, together with the leading m_t^4 -term, which constitutes a very poor approximation.

Pure fermion-loop contributions (n fermion loops at n -loop order) have also been investigated^{63,64}. In the on-shell scheme, explicit results have been worked out up to 4-loop order, which allows an investigation of the validity of the resummation (20) for the non-leading 2-loop and higher-order terms. It was found that numerically the resummation (20) works remarkably well, within 2 MeV in M_W .

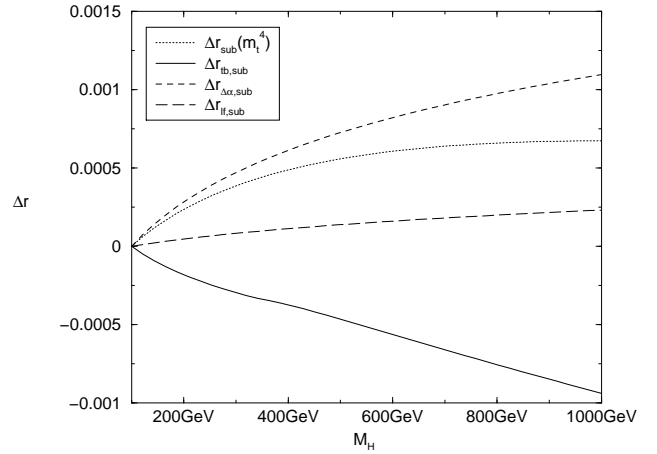


Figure 2: Higgs mass dependence of fermionic contributions to Δr at the two-loop level (from⁶³). The different curves show the various contributions: light fermions via $\Delta\alpha$ ($\Delta r_{\Delta\alpha}$), residual light-fermion contribution not in $\Delta\alpha$ (Δr_{lf}), the contribution from the (tb) doublet (Δr_{tb}), and the approximation of the (tb) two-loop contribution by the term proportional to m_t^4 . Displayed in each case is the difference $\Delta r(M_H) - \Delta r(100 \text{ GeV})$.

2.3 Z boson observables

Measurements of the Z line shape in $e^+e^- \rightarrow f\bar{f}$ yield the parameters M_Z , Γ_Z , and the partial widths Γ_f or the peak cross section

$$\sigma_0^f = \frac{12\pi}{M_Z^2} \cdot \frac{\Gamma_e \Gamma_f}{\Gamma_Z^2}. \quad (21)$$

Angular distributions and polarization measurements of the final fermions yield forward–backward and polarization asymmetries. Whereas M_Z is used as a precise input parameter, together with α and G_μ , the width, partial widths and asymmetries allow comparisons with the predictions of the standard model. The predictions for the partial widths as well as for the asymmetries can conveniently be calculated in terms of effective neutral current coupling constants for the various fermions.

Effective Z boson couplings: The effective couplings follow from the set of 1-loop diagrams without virtual photons, the non-QED or weak corrections. These weak corrections can conveniently be written in terms of fermion-dependent overall normalizations ρ_f and effective mixing angles s_ℓ^2 in the NC vertices (see e.g. ⁶⁵):

$$\begin{aligned} J_\nu^{\text{NC}} &= \left(\sqrt{2}G_\mu M_Z^2\right)^{1/2} (g_V^f \gamma_\nu - g_A^f \gamma_\nu \gamma_5) \quad (22) \\ &= \left(\sqrt{2}G_\mu M_Z^2 \rho_f\right)^{1/2} \left((I_3^f - 2Q_f s_\ell^2)\gamma_\nu - I_3^f \gamma_\nu \gamma_5\right). \end{aligned}$$

ρ_f and s_ℓ^2 contain universal parts, e.g. from the ρ -parameter via

$$\rho_f = \frac{1}{1 - \Delta\rho} + \dots, \quad s_\ell^2 = s_W^2 + c_W^2 \Delta\rho + \dots \quad (23)$$

with $\Delta\rho$ from Eq. (13) and non-universal parts that explicitly depend on the type of the external fermions.

The subleading 2-loop corrections $\sim G_\mu^2 m_t^2 M_Z^2$ for the leptonic mixing angle ⁶¹ s_ℓ^2 have also been obtained in the meantime, as well as for ρ_ℓ ⁶⁶.

Meanwhile exact results have been derived for the Higgs-dependence of the fermionic 2-loop corrections in s_ℓ^2 ^{63,64}, and comparisons were performed with those obtained via the top mass expansion ⁶³. Differences in the values of s_ℓ^2 can amount to $0.8 \cdot 10^{-4}$ when M_H is varied over the range from 100 GeV to 1 TeV.

Figure 3 shows the Higgs-mass dependence of the 2-loop corrections to s_ℓ^2 associated with the t/b doublet, with $\Delta\alpha$, and with the light fermion terms not in $\Delta\alpha$. As can be seen, the M_H -dependence of the light fermions yields contributions to s_ℓ^2 up to $2 \cdot 10^{-5}$. For ρ_ℓ or equivalently the leptonic Z widths, the subleading 2-loop effects are small, and differences with the results in the top mass dependence are irrelevant.

For the b quark coupling to the Z boson, not only the universal contribution through the ρ -parameter but also the non-universal parts have a strong dependence on m_t , resulting from virtual top quarks in the vertex corrections. The difference between the d and b couplings can be parametrized in the following way

$$\rho_b = \rho_d(1 + \tau)^2, \quad s_b^2 = s_d^2(1 + \tau)^{-1}, \quad (24)$$

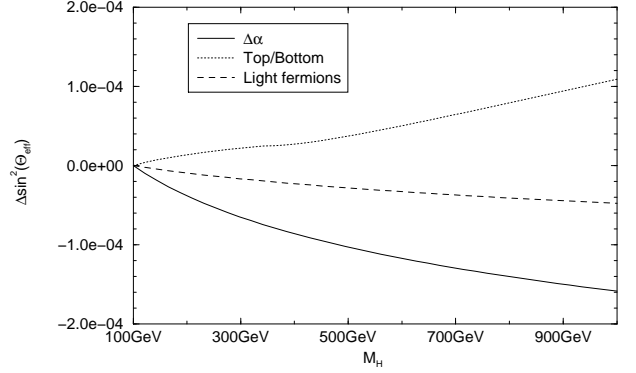


Figure 3: Higgs mass dependence of the various fermionic contributions at the two-loop level to the effective leptonic mixing angle s_ℓ^2 at the Z peak: light fermion contribution via $\Delta\alpha$, light fermion contribution not in $\Delta\alpha$, and the contribution from the (tb) doublet. Shown in each case is the difference $s_\ell^2(M_H) - s_\ell^2(100 \text{ GeV})$.

with the quantity

$$\tau = \Delta\tau^{(1)} + \Delta\tau^{(2)} + \Delta\tau^{(\alpha_s)}$$

calculated perturbatively, including the complete 1-loop order term ⁶⁷ with x_t from Eq. (14):

$$\Delta\tau^{(1)} = -2x_t - \frac{G_\mu M_Z^2}{6\pi^2 \sqrt{2}} (c_W^2 + 1) \log \frac{m_t}{M_W} + \dots, \quad (25)$$

and the leading electroweak 2-loop contribution of $O(G_\mu^2 m_t^4)$ ^{46,68}

$$\Delta\tau^{(2)} = -2x_t^2 \tau^{(2)}, \quad (26)$$

where $\tau^{(2)}$ is a function of M_H/m_t with $\tau^{(2)} = 9 - \pi^2/3$ for small M_H .

Asymmetries and mixing angles: The effective mixing angles are of particular interest, since they determine the on-resonance asymmetries via the combinations

$$A_f = \frac{2g_V^f g_A^f}{(g_V^f)^2 + (g_A^f)^2}, \quad (27)$$

namely

$$A_{\text{FB}} = \frac{3}{4} A_e A_f, \quad A_\tau^{\text{pol}} = A_\tau, \quad A_{\text{LR}} = A_e. \quad (28)$$

Measurements of the asymmetries hence are measurements of the ratios

$$g_V^f/g_A^f = 1 - 2Q_f s_\ell^2 \quad (29)$$

or the effective mixing angles, respectively.

Z width and partial widths: The total Z width Γ_Z can be calculated essentially as the sum over the fermionic partial decay widths. Expressed in terms of the effective coupling constants, they read up to second order in the fermion masses:

$$\Gamma_f = \Gamma_0 \left[(g_V^f)^2 + (g_A^f)^2 \left(1 - \frac{6m_f^2}{M_Z^2} \right) \right] \cdot \left(1 + Q_f^2 \frac{3\alpha}{4\pi} \right) + \Delta\Gamma_{\text{QCD}}^f$$

with

$$\Gamma_0 = N_C^f \frac{\sqrt{2}G_\mu M_Z^3}{12\pi}, \quad N_C^f = 1 \text{ (leptons)}, = 3 \text{ (quarks)}.$$

The QCD correction for the light quarks with $m_q \simeq 0$ is given by

$$\Delta\Gamma_{\text{QCD}}^f = \Gamma_0 \left((g_V^f)^2 + (g_A^f)^2 \right) \cdot K_{\text{QCD}} \quad (30)$$

with⁶⁹

$$K_{\text{QCD}} = \frac{\alpha_s}{\pi} + 1.41 \left(\frac{\alpha_s}{\pi} \right)^2 - 12.8 \left(\frac{\alpha_s}{\pi} \right)^3 - \frac{Q_f^2 \alpha \alpha_s}{4 \pi^2}.$$

For b quarks the QCD corrections are different, because of finite b mass terms and to top-quark-dependent 2-loop diagrams for the axial part:

$$\Delta\Gamma_{\text{QCD}}^b = \Delta\Gamma_{\text{QCD}}^d + \Gamma_0 \left[(g_V^b)^2 R_V + (g_A^b)^2 R_A \right]. \quad (31)$$

The coefficients in the perturbative expansions

$$R_V = c_1^V \frac{\alpha_s}{\pi} + c_2^V \left(\frac{\alpha_s}{\pi} \right)^2 + c_3^V \left(\frac{\alpha_s}{\pi} \right)^3 + \dots, \\ R_A = c_1^A \frac{\alpha_s}{\pi} + c_2^A \left(\frac{\alpha_s}{\pi} \right)^2 + \dots$$

depending on m_b and m_t , are calculated up to third order in α_s , except for the m_b -dependent singlet terms, which are known to $O(\alpha_s^2)$ ^{70,71}. For a review of the QCD corrections to the Z width, see⁷².

The partial decay rate into b -quarks, in particular the ratio $R_b = \Gamma_b/\Gamma_{\text{had}}$, is an observable of special sensitivity to the top quark mass. Therefore, beyond the pure QCD corrections, also the 2-loop contributions of the mixed QCD–electroweak type, are important. The QCD corrections were first derived for the leading term of $O(\alpha_s G_\mu m_t^2)$ ⁷³ and were subsequently completed by the $O(\alpha_s)$ correction to the $\log m_t/M_W$ term⁷⁴ and the residual terms of $O(\alpha\alpha_s)$ ⁷⁵.

In the same spirit, also the complete 2-loop $O(\alpha\alpha_s)$ to the partial widths into the light quarks have been obtained, beyond those that are already contained in the factorized expression (30) with the electroweak 1-loop couplings⁷⁶. These “non-factorizable” corrections yield

an extra negative contribution of $-0.55(3)$ MeV to the total hadronic Z width (converted into a shift of the strong coupling constant, they correspond to $\delta\alpha_s = 0.001$). In summary, the 2-loop corrections of $O(\alpha\alpha_s)$ to the electroweak precision observables are by now completely under control. More details can be found in⁵⁴.

Radiation of secondary fermions through photons from the primary final state fermions can yield another sizeable contribution to the partial Z widths; however, this is compensated by the corresponding virtual contribution through the dressed photon propagator in the final-state vertex correction for sufficiently inclusive final states, i.e. for loose cuts to the invariant mass of the secondary fermions⁷⁷.

QED corrections: The observed cross section is the result of convoluting the cross section for $e^+e^- \rightarrow f\bar{f}$ calculated on the basis of the effective couplings with the initial-state QED corrections consisting of virtual photon and real photon bremsstrahlung contributions:

$$\sigma_{\text{obs}}(s) = \int_0^{k_{\text{max}}} dk H(k) \sigma(s(1-k)); \quad (32)$$

k_{max} denotes a cut to the radiated energy. Kinematically it is limited by $1 - 4m_f^2/s$ or $1 - 4m_\pi^2/s$ for hadrons, respectively. For the required accuracy, multiphoton radiation has to be included. The radiator function $H(k)$ with soft-photon resummation and the exact $O(\alpha^2)$ result for initial-state QED corrections is given in ref⁷⁸. It has been improved recently by the $O(\alpha^3)$ term⁷⁹.

Bhabha scattering in the forward direction is the crucial theoretical tool for the determination of the luminosity and therefore requires a careful treatment, including higher-order QED corrections⁸⁰. Improvements in the calculation of the $O(\alpha^2)$ next-to-leading logarithmic contributions in the Monte Carlo generator BHLUMI are an important step in pinning down the theoretical error from 0.11% to 0.06%⁸¹.

2.4 Accuracy of the standard model predictions

For a discussion of the theoretical reliability of the standard model predictions, one has to consider the various sources contributing to their uncertainties:

Parametric uncertainties result from the limited precision in the experimental values of the input parameters, essentially $\alpha_s = 0.119 \pm 0.002$ ⁵³, $m_t = 173.8 \pm 5.0$ GeV⁵, $m_b = 4.7 \pm 0.2$ GeV, and the hadronic vacuum polarization as discussed in section 2.1. The conservative estimate of the error in Eq. (10) leads to $\delta M_W = 13$ MeV in the W -mass prediction, and $\delta \sin^2 \theta = 0.00023$ common to all of the mixing angles.

The uncertainties from the QCD contributions can essentially be traced back to those in the top quark loops

in the vector boson self-energies. The knowledge of the $O(\alpha_s^2)$ corrections to the ρ -parameter and Δr yields a significant reduction; they are small, although not negligible (e.g. $\sim 3 \cdot 10^{-5}$ in s_ℓ^2).

The size of unknown higher-order contributions can be estimated by different treatments of non-leading terms of higher order in the implementation of radiative corrections in electroweak observables (‘options’) and by investigations of the scheme dependence. Explicit comparisons between the results of 5 different computer codes based on on-shell and \overline{MS} calculations for the Z -resonance observables are documented in the ‘‘Electroweak Working Group Report’’⁶⁵ in ref²⁶. The inclusion of the non-leading 2-loop corrections $\sim G_\mu^2 m_t^2 M_Z^2$ reduce the uncertainty in M_W below 10 MeV and in s_ℓ^2 below 10^{-4} , typically to $\pm 4 \cdot 10^{-5}$.

3 Standard model and precision data

We now confront the standard model predictions for the discussed set of precision observables with the most recent sample of experimental data^{1,2}. In table 1 the standard model predictions for Z -pole observables and the W mass are put together for the best fit input data set, given in (34). The experimental results on the Z observables are from LEP and the SLC, the W mass is from combined LEP and $p\bar{p}$ data. The leptonic mixing angle determined via A_{LR} by the SLD experiment⁸² and the s_ℓ^2 average from LEP:

$$s_\ell^2(A_{LR}) = 0.23109 \pm 0.00029$$

$$s_\ell^2(\text{LEP}) = 0.23189 \pm 0.00024$$

have come closer to each other in their central value; owing to their smaller errors, however, they still differ by 2.8 standard deviations.

Table 1 contains the combined LEP/SLD value. ρ_ℓ and s_ℓ^2 are the leptonic neutral current couplings in Eq. (22), derived from partial widths and asymmetries under the assumption of lepton universality.

Note that the experimental value for ρ_ℓ points at the presence of genuine electroweak corrections by 3.5 standard deviations. In s_ℓ^2 the presence of purely bosonic radiative corrections is clearly established when the experimental result is compared with a theoretical value containing only the fermion loop corrections, an observation that has been persisting already for several years⁸³. The deviation from the standard model prediction in the quantity R_b has been reduced below one standard deviation by now. Other small deviations are observed in the asymmetries: the purely leptonic A_{FB} is slightly higher than the standard model predictions, and A_{FB} for b quarks is lower. Whereas the leptonic A_{FB} favours a

Table 1: Precision observables: experimental results from combined LEP and SLD data for Z observables and combined $p\bar{p}$ and LEP data for M_W , together with the standard model predictions for the best fit, i.e. for the parameter values given in Eq. (34). ρ_ℓ and s_ℓ^2 are derived from the experimental values of $g_{V,A}^\ell$ according to Eq. (22), averaged under the assumption of lepton universality.

Observable	Exp.	SM best fit
M_Z (GeV)	91.1867 ± 0.0019	91.1865
Γ_Z (GeV)	2.4939 ± 0.0024	2.4956
σ_0^{had} (nb)	41.491 ± 0.058	41.476
R_{had}	20.765 ± 0.026	20.745
R_b	0.21656 ± 0.00074	0.2159
R_c	0.1732 ± 0.0048	0.1722
A_{FB}^ℓ	0.01683 ± 0.00096	0.0162
A_{FB}^b	0.0990 ± 0.0021	0.1029
A_{FB}^c	0.0709 ± 0.0044	0.0735
A_b	0.867 ± 0.035	0.9347
A_c	0.647 ± 0.040	0.6678
ρ_ℓ	1.0041 ± 0.0012	1.0051
s_ℓ^2	0.23157 ± 0.00018	0.23155
M_W (GeV)	80.39 ± 0.06	80.372

very light Higgs boson, the b quark asymmetry needs a heavy Higgs.

The effective mixing angle is an observable most sensitive to the mass M_H of the Higgs boson. Since a light Higgs boson corresponds to a low value of s_ℓ^2 , the strongest upper bound on M_H is from A_{LR} at the SLC⁸². The inclusion of the two-loop electroweak corrections $\sim m_t^2$ from⁶¹ yields a sizeable positive contribution to s_ℓ^2 , see Figure 4. The inclusion of this term hence strengthens the upper bound on M_H .

The W mass prediction in table 1 is obtained from Eq. (18) (including the higher-order terms) from M_Z, G_μ, α and M_H, m_t . The present experimental value for the W mass from the combined LEP 2, UA2, CDF and D0 results is in best agreement with the standard model prediction.

The quantity s_W^2 resp. the ratio M_W/M_Z can indirectly be measured in deep-inelastic neutrino–nucleon scattering. The average from the experiments CCFR, CDHS and CHARM⁸⁵ with the recent NUTEV result⁸⁶

$$s_W^2 = 1 - M_W^2/M_Z^2 = 0.2255 \pm 0.0021 \quad (33)$$

for $m_t = 175$ GeV and $M_H = 150$ GeV corresponds to $M_W = 80.25 \pm 0.11$ GeV and is hence fully consistent with the direct vector boson mass measurements and with the standard theory.

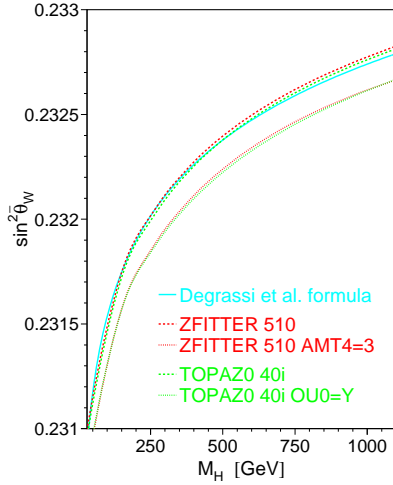


Figure 4: Higgs mass dependence of s_ℓ^2 with and without the electroweak 2-loop term $\sim m_t^2$, comparison of ZFITTER and TOPAZ0 codes. The lower sample of curves is without, the upper sample with the 2-loop term (figure prepared by C. Pauss).

Standard model global fits: The FORTRAN codes ZFITTER⁸⁷ and TOPAZ0⁸⁸ have been updated by incorporating all the recent precision calculation results that were discussed in the previous section. Comparisons have shown good agreement between the predictions from the two independent programs⁸⁹. Global fits of the standard model parameters to the electroweak precision data done by the Electroweak Working Group¹ are based on these recent versions. Including m_t and M_W from the direct measurements in the experimental data set, together with s_W^2 from neutrino scattering, the standard model parameters for the best fit result are:

$$\begin{aligned} m_t &= 171.1 \pm 4.9 \text{ GeV} \\ M_H &= 76_{-47}^{+85} \text{ GeV} \\ \alpha_s &= 0.119 \pm 0.003. \end{aligned} \quad (34)$$

The upper limit to the Higgs mass at the 95% C.L. is $M_H < 262$ GeV, where the theoretical uncertainty is included. Thereby the hadronic vacuum polarization in Eq. (10) has been used (solid line in Figure 6). With the theory-driven result on $\Delta\alpha_{\text{had}}$ of ref³³ one obtains¹ $M_H = 92_{-41}^{+64}$ (dashed line). The 1σ upper bound on M_H is influenced only marginally. The reason is that simultaneously with the error reduction the central value of M_H is shifted upwards (see Figure 6). Another recent analysis⁹⁰ (for earlier studies see^{91,92}) based on the data set of summer 1998 yields a Higgs mass $M_H = 107_{-45}^{+67}$ GeV. About one half of the difference with (34) can be ascribed to the use of $\alpha(M_Z)$ of ref³⁷, which is very

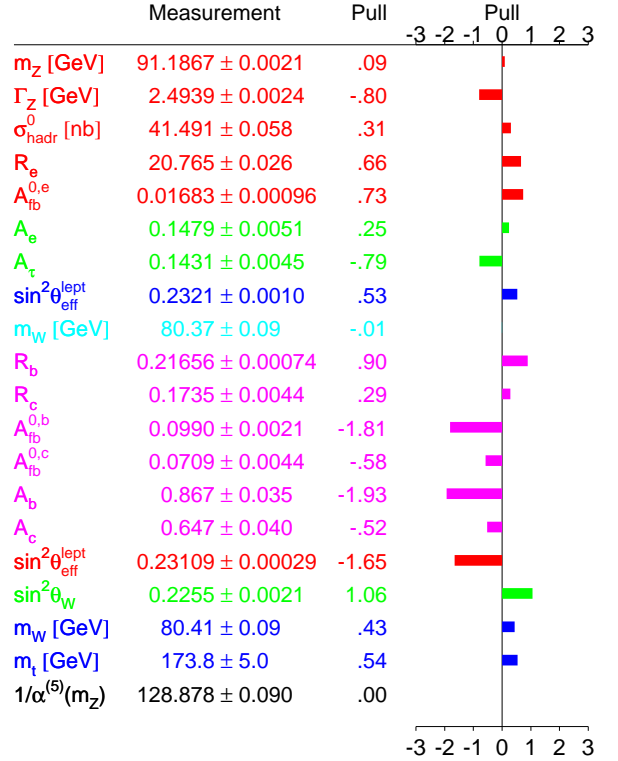


Figure 5: Experimental results and pulls from a standard model fit (from ref^{1,2}). pull = obs(exp)-obs(SM)/(exp.error).

close to the value in ref^{33,35}; the residual shift might be interpreted as due to different renormalization schemes and different treatments of α_s .

With an overall $\chi^2/\text{d.o.f.} = 15/15$ the quality of the fit is remarkably high. As can be seen from Figure 5, the deviation of the individual quantities from the standard model best-fit values are below 2 standard deviations.

Compared with the results from 1997, the central value for the Higgs mass has moved to lower values and the error has been decreased. The Higgs mass bounds follow from the χ^2 distribution shown in Figure 6. The shift in the central value can be understood from Figure 7, which illustrates the effect of the inclusion of the electroweak two-loop contribution by Degrassi et al.⁶¹, which was not implemented in the codes for the analysis in 1997. Since it increases the prediction for s_ℓ^2 (Figure 4) for a given Higgs mass, the allowed values of M_H are shifted accordingly downwards.

The second observation is the decrease of the error, which besides the experimental improvements results from the reduction of the theoretical uncertainties of pure electroweak origin. The shaded band around the solid line in Figure 6 is the influence of the various ‘options’

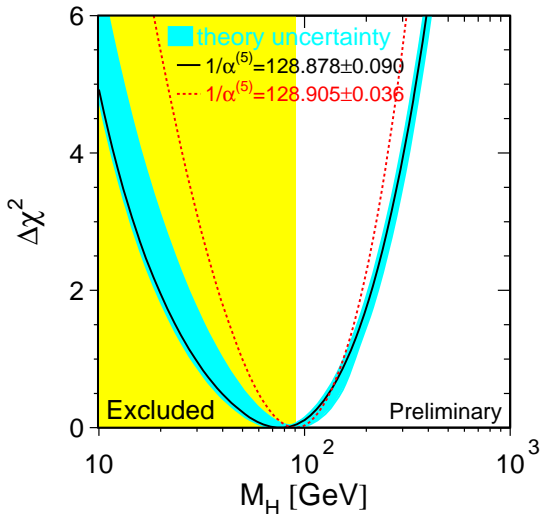


Figure 6: Higgs mass dependence of χ^2 in the global fit to precision data (from ref^{1,2}). The shaded band displays the error from the theoretical uncertainties obtained from various options in the codes ZFITTER and TOPAZ0.

(see section 2.4) in the codes ZFITTER and TOPAZ0 after the implementation of the 2-loop electroweak terms $\sim m_t^2$. It is thus the direct continuation of the error estimate done in the previous study⁶⁵. Compared with the width of the uncertainty band in 1997¹ the shrinking is evident.

On the other hand, the remaining theoretical uncertainty associated with the Higgs mass bounds should be taken very seriously. The effect of the inclusion of the next-to-leading term in the m_t -expansion of the electroweak 2-loop corrections in the precision observables has shown to be sizeable, at the upper margin of the estimate given in⁶⁵. It is thus not guaranteed that the subsequent subleading terms in the m_t -expansion are indeed smaller in size. Kühn⁵⁴ has given an example for an explicit calculation where the subleading terms of the m_t -expansion are of comparable size and tend to cancel each other. Also the variation of the M_H -dependence at different stages of the calculation, as discussed in sections 2.2 and 2.3, indicate the necessity of more complete results at two-loop order. Having in mind also the variation of the Higgs mass bounds under the fluctuations of the experimental data², the limits for M_H derived from the analysis of electroweak data in the frame of the standard model still carry a noticeable uncertainty. Nevertheless, as a central message, it can be concluded that the indirect determination of the Higgs mass range has shown that the Higgs is light, with its mass well below the non-perturbative regime.

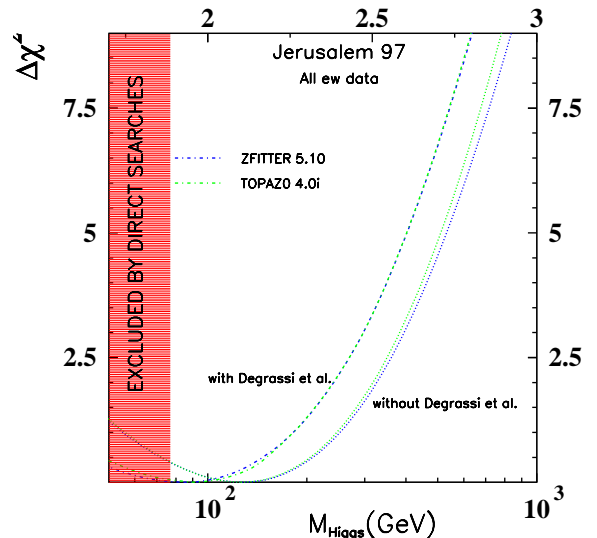


Figure 7: Higgs mass dependence of χ^2 in the global fit to precision data with and without the 2-loop term (figure prepared by G. Quast).

4 Production and decay of W bosons

The success of the standard model in the correct description of the electroweak precision observables is simultaneously an indirect confirmation of the Yang–Mills structure of the gauge boson self-interaction. For conclusive confirmations the direct experimental investigation is required. At LEP 2 (and higher energies), pair production of on-shell W bosons can be studied experimentally, allowing tests of the trilinear vector boson self-couplings and precise M_W measurements. For LEP 2, an error of about 40 MeV in M_W can be reached⁹³. For this purpose standard model calculations for the process $e^+e^- \rightarrow W^+W^- \rightarrow 4f$ and the corresponding 4-fermion background processes are mandatory at the accuracy level of at least 1%. This requires the understanding of the radiative corrections to the W boson production and decay processes, as well as a careful treatment of the finite-widths effects.

For practical purposes, improved Born approximations are in use for both resonating and non-resonating processes, dressed by initial-state QED corrections. A status report can be found in ref⁹⁴. QED corrections with soft photon exponentiation to unstable W pair production are implemented in Monte Carlo generators⁹⁵.

One of the specific problems in the theoretical description of the production process for W bosons is the presence of the width term in the W propagator, which violates gauge invariance, yielding gauge-dependent am-

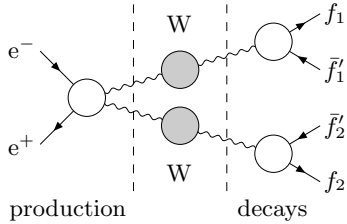


Figure 8: The generic structure of the factorizable W -pair contributions. The shaded circles indicate the Breit–Wigner resonances.

plitudes. As a solution, it has been proposed⁹⁶ to take into account also the imaginary part in the $WW\gamma$ vertex from the light fermion triangle loops (see also⁹⁷). This prescription is in accordance with gauge invariance and cures the Ward identities between 2- and 3-point functions involving W^\pm and γ . This scheme can be extended to incorporating the whole set of fermion loop contributions at the one-loop level in the double- and single-resonating processes⁹⁸.

The systematic treatment of the complete radiative corrections is a task of enormous complexity. A reasonable simplification is given in terms of the double-pole approximation with two resonating W bosons, the accuracy of which is estimated to be of order 0.1% if one is not too close to the WW threshold⁹⁹. The ‘factorizable corrections’, displayed in Figure 8, can be attributed either to the production of the gauge boson pair or to the subsequent decays. In the other class of ‘non-factorizable corrections’ the diagrams cannot be separated into a production process and decay processes (Figure 9). There are two recent independent calculations of the non-factorizable corrections in the double-pole approximation^{100,101}, with very good agreement. Their effect on the invariant mass distribution of one of the decaying W ’s is below 1% for energies above 180 GeV. An example is shown in Figure 10, where the single invariant-mass distribution $d\sigma/dM_1$ is displayed for the process $e^+e^- \rightarrow WW \rightarrow e^+\nu_e e^-\bar{\nu}_e$. The signatures are very similar also for other decay channels. In the inclusive cross sections, the non-factorizable terms are zero in the double-pole approximation¹⁰².

In the case of 4-quark final states, diagrams similar to those in Figure 9 arise, with the photon between two fermions replaced by a gluon line. Such typical non-factorizable QCD corrections are only formally analogous to the QED ones: in the soft-gluon limit, which is required to maintain the double-pole structure of the amplitude, the strong interaction becomes non-perturbative and can thus not be dealt with in terms of Feynman diagrams. This ‘colour reconnection’ leads to a distortion of the individual hadronic systems from separated W de-

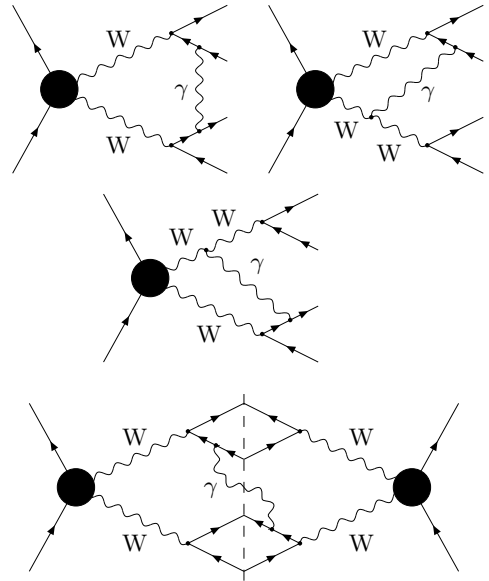


Figure 9: Examples of virtual (top) and real (bottom) non-factorizable corrections to W -pair production.

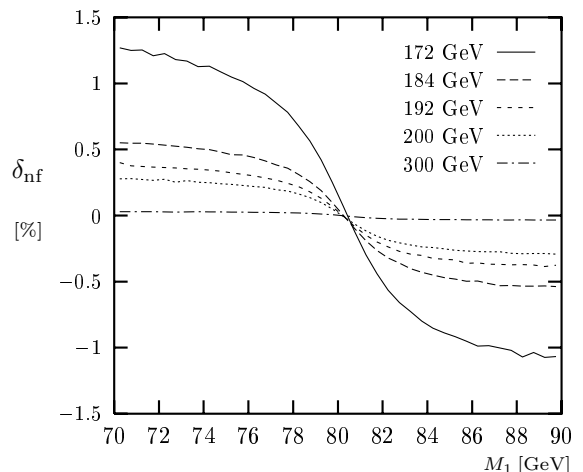


Figure 10: Relative non-factorizable corrections to the single-invariant-mass distribution in the process $e^+e^- \rightarrow WW \rightarrow e^+\nu_e e^-\bar{\nu}_e$. From ref¹⁰¹.

cays and can at present be treated only with the help of hadronization models. It yields the dominant systematic error in the W mass reconstruction from 4-jet final states and is mainly responsible for the limited accuracy of about 40 MeV in the W -mass measurement at LEP.

Production of single- W resonances occurs as a Drell–Yan process $qq' \rightarrow W \rightarrow \ell^+ \nu_\ell$ in hadron collisions. Run II of the upgraded Tevatron will provide precision measurements of M_W , comparable to that at LEP or even more accurate. For this purpose the inclusion of the complete set of one-loop electroweak corrections to the resonating Drell–Yan process^{103,104} becomes necessary. The electroweak radiative corrections to the W propagator around the resonance have also been studied in¹⁰⁵.

5 The Higgs sector

The minimal model with a single scalar doublet is the simplest way to implement the electroweak symmetry breaking. The experimental result that the ρ -parameter is very close to unity is a natural feature of models with doublets and singlets. In the standard model, the mass M_H of the Higgs boson appears as the only additional parameter beyond the vector boson and fermion masses. M_H cannot be predicted but has to be taken from experiment. The present lower limit (95% C.L.) from the search at LEP¹⁰⁶ is 89 GeV. Indirect determinations of M_H from precision data have already been discussed in section 3. The indirect mass bounds react sensitively to small changes in the input data, which is a consequence of the logarithmic dependence of electroweak precision observables. As a general feature, it appears that the data prefer a light Higgs boson.

There are also theoretical constraints on the Higgs mass from vacuum stability and absence of a Landau pole^{107,108,109}, and from lattice calculations¹¹⁰. Explicit perturbative calculations of the decay width for $H \rightarrow W^+W^-, ZZ$ in the large- M_H limit in 2-loop order¹¹² have shown that the 2-loop contribution exceeds the 1-loop term in size (same sign) for $M_H > 930$ GeV (Figure 11). This result is confirmed by the calculation of the next-to-leading order correction in the $1/N$ expansion, where the Higgs sector is treated as an $O(N)$ symmetric σ -model¹¹³. A similar increase of the 2-loop perturbative contribution with M_H is observed for the fermionic decay¹¹⁴ $H \rightarrow f\bar{f}$, but with opposite sign leading to a cancellation of the one-loop correction for $M_H \simeq 1100$ GeV (Figure 11). The requirement of applicability of perturbation theory therefore puts a stringent upper limit on the Higgs mass. The indirect Higgs mass bounds obtained from the precision analysis show, however, that the Higgs boson is well below the mass range where the Higgs sector becomes non-perturbative. The

lattice result¹¹¹ for the bosonic Higgs decay in Figure 11 for $M_H = 727$ GeV is not far from the perturbative 2-loop result. The difference may at least partially be interpreted as missing higher-order terms.

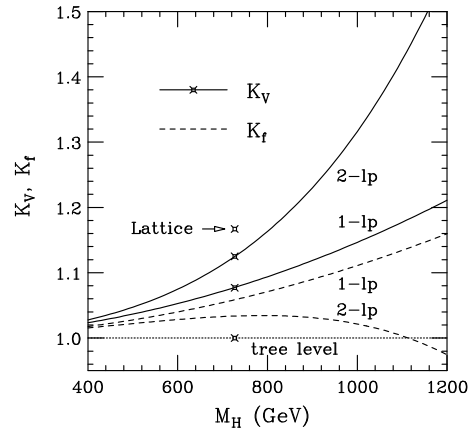


Figure 11: Correction factors for the Higgs decay widths $H \rightarrow VV$ ($V = W, Z$) and $H \rightarrow f\bar{f}$ in 1- and 2-loop order (from ref¹¹⁵)

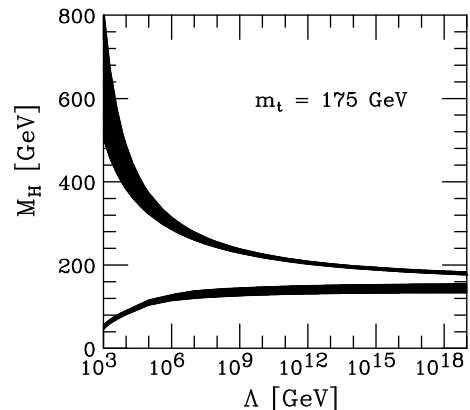


Figure 12: Theoretical limits on the Higgs boson mass from the absence of a Landau pole and from vacuum stability (from ref¹⁰⁹)

The behaviour of the quartic Higgs self-coupling λ , as a function of a rising energy scale μ , follows from the renormalization group equation with the β -function dominated by λ and the top quark Yukawa coupling g_t contributions:

$$\beta_\lambda = 24\lambda^2 + 12\lambda g_t^2 - 6g_t^4 + \dots \quad (35)$$

In order to avoid unphysical negative quartic couplings from the negative top quark contribution, a lower bound on the Higgs mass is derived. The requirement that the Higgs coupling remains finite and positive up to a scale Λ yields constraints on the Higgs mass M_H , which have been evaluated at the 2-loop level^{108,109}. These bounds on M_H are shown in Figure 12 as a function of the cut-off scale Λ up to which the standard Higgs sector can be

extrapolated, for $m_t = 175$ GeV and $\alpha_s(M_Z) = 0.118$. The allowed region is the area between the lower and the upper curves. The bands indicate the theoretical uncertainties associated with the solution of the renormalization group equations¹⁰⁹. It is interesting to note that the indirect determination of the Higgs mass range from electroweak precision data via radiative corrections is compatible with a value of M_H where Λ can extend up to the Planck scale.

6 The standard model at lower energies

6.1 The decay $B \rightarrow X_s \gamma$

The rare radiative decay processes $B \rightarrow X_s \gamma$ are mediated by loop diagrams and hence represent sensitive probes of the standard model as well as of extensions such as 2-Higgs doublet models or supersymmetric models. In the standard model the next-to-leading QCD calculation for the total branching ratio has been completed¹¹⁶, which together with the electroweak corrections¹¹⁷ yields as the present best standard model prediction (for a recent review see¹¹⁸):

$$B(B \rightarrow X_s \gamma)_{\text{theor}} = (3.29 \pm 0.33) \cdot 10^{-4}. \quad (36)$$

From the experimental side, the CLEO Collaboration has reported a new result:¹¹⁹ $B(B \rightarrow X_s \gamma) = (3.15 \pm 0.35 \pm 0.32 \pm 0.26) \cdot 10^{-4}$; the corresponding result by ALEPH¹²⁰ from B mesons produced at the Z resonance is $B(B \rightarrow X_s \gamma) = (3.11 \pm 0.80 \pm 0.72) \cdot 10^{-4}$. The experimental results are very close to each other and agree remarkably well with the standard model prediction (36). This further confirmation of the standard model simultaneously puts stringent limits to potential New Physics beyond the standard model¹²¹.

6.2 Muon anomalous magnetic moment

The anomalous magnetic moment of the muon,

$$a_\mu = \frac{g_\mu - 2}{2} \quad (37)$$

provides a precision test of the standard model at low energies. Within the present experimental accuracy⁵³ of $\Delta a_\mu = 840 \cdot 10^{-11}$, theory and experiment are in best agreement, but the electroweak loop corrections are still hidden in the noise. The new experiment E 821 at the Brookhaven National Laboratory¹²² is designed to reduce the experimental error down to 40 ± 10^{-11} and hence will become sensitive to the electroweak loop contribution.

For this reason the standard model prediction has to be known with at least comparable precision. Recent theoretical work in this direction has provided the

electroweak 2-loop terms^{124,125} with 3-loop leading-logarithmic contributions¹²⁶ and updated the contribution from the hadronic photonic vacuum polarization^{29,127,32,33}, which is visualized in Figure 13. The lowest data point with the smallest error³³ is obtained with the help of the theory-driven QCD analysis, which has been applied also to $\Delta\alpha_{\text{had}}(M_Z)$ (see section 2.1).

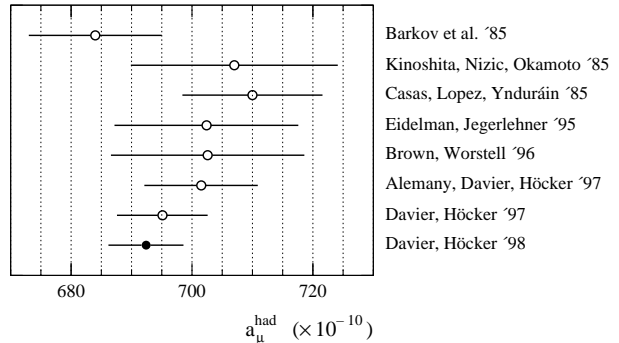


Figure 13: Various determinations of a_μ^{had} (from ref³⁴)

The main sources of the theoretical error at present are the hadronic vacuum polarization and the light-by-light scattering mediated by quarks, as part of the 3-loop hadronic contribution^{128,129,130}. Table 3 contains the breakdown of a_μ . The hadronic part is supplemented by the higher-order α^3 vacuum polarization effects¹³¹ (included in the numerical value), but it does not include the light-by-light scattering contribution, which is listed separately in the table.

Table 2: Contributions Δa_μ to the muonic anomalous magnetic moment and their theoretical uncertainties, in units of 10^{-11} .

Source	Δa_μ	Error
QED ¹³²	116584706	2
Hadronic ^{29,131}	6916	153
Hadronic ³³	6816	62
EW, 1-loop ¹²³	195	
EW, 2-loop ¹²⁵	-44	4
Light-by-light ¹²⁹	-79	15
Light-by-light ¹³⁰	-92	32
Exp. (future)		40

The 2-loop electroweak contribution is as large as the expected experimental error. The dominating theoretical uncertainty at present is still the error in the hadronic vacuum polarization. The previous discrepancy in the contribution involving light-by-light scattering has been removed, with the consequence that this term can now be considered as established with an acceptable uncertainty.

7 Beyond the standard model

7.1 Conceptual problems

The comparison of the theoretical predictions with experimental data has confirmed the validity of the standard model in an impressive way:

- the description of the data is nearly perfect, with no significant indication for deviations;
- the quantum effects of the standard model have been established at the level of several σ ;
- direct and indirect determinations of the top quark mass are compatible with each other;
- the Higgs boson mass is meanwhile also being constrained within the perturbative mass regime with the possibility that the standard model may be extrapolated up to energies around the Planck scale.

In spite of this success, the conceptual situation with the standard model is unsatisfactory for quite a few deficiencies:

- the smallness of the electroweak scale $v \sim 246 \text{ GeV} \ll M_{\text{Pl}}$ (the ‘hierarchy problem’);
- the large number of free parameters (gauge couplings, vacuum expectation value, M_H , fermion masses, CKM matrix elements), which are not predicted but have to be taken from experiments;
- the pattern that occurs in the arrangement of the fermion masses;
- the missing way to connect to gravity.

It is a curiosity of the standard model that these questions will persist even after the Higgs boson will have been discovered.

7.2 Massive neutrinos

Besides the long-standing list of conceptual theoretical problems, a new perspective arises through the recent experimental results by Super-Kamiokande¹³⁴ on the atmospheric neutrino anomaly, which can most easily be explained by oscillations between different ν species, associated with neutrino masses different from zero. In the strict-minimal model, neutrinos are massless and right-handed neutrino components are absent. The evidence for massive neutrinos requires a modification of the minimal model in order to accommodate neutrinos with mass. The straightforward way to introduce mass terms is the augmentation of the fermion sector by right-handed partners ν_R ; together with the familiar ν_L these allow the presence of Dirac mass terms $\sim m_\nu \bar{\nu} \nu$ with $\nu = \nu_L + \nu_R$ and m_ν as additional mass parameters, without altering the global architecture of the standard model and without spoiling the successful description of all the other electroweak phenomena. What appears unsatisfactory is the unexplained smallness of the neutrino Dirac masses,

as enforced by the empirical situation. A commonly accepted elegant solution is given by the seesaw-mechanism where a lepton-number-violating Majorana mass term $\sim M$ is introduced. Together with the Dirac mass, which is of the order of the usual charged lepton masses, a very light and a very heavy ν component appear with the light one almost entirely left-handed, when M is of the order of the GUT scale. Candidates for specific models are Grand Unification scenarios such as the SO(10)-GUT, where ν_R fits into the same 16-dimensional representation as the other fermions of a family. Hence, the appearance of small neutrino masses points towards a new high-mass scale beyond the minimal model, which may be associated with the concept of further unification of the fundamental forces.

7.3 The minimal supersymmetric standard model (MSSM)

Among the extensions of the standard model, the MSSM is the theoretically favoured scenario as the most predictive framework beyond the standard model. A definite prediction of the MSSM is the existence of a light Higgs boson with mass below $\sim 135 \text{ GeV}$ ¹³⁵. The detection of a light Higgs boson at LEP could be a significant hint for supersymmetry.

The structure of the MSSM as a renormalizable quantum field theory allows a similarly complete calculation of the electroweak precision observables as in the standard model in terms of one Higgs mass (usually taken as the CP -odd ‘pseudoscalar’ mass M_A) and $\tan\beta = v_2/v_1$, together with the set of SUSY soft-breaking parameters fixing the chargino/neutralino and scalar fermion sectors. It has been known for quite some time¹³⁶ that light non-standard Higgs bosons as well as light stop and charginos predict larger values for the ratio R_b ^{137,139}. Complete 1-loop calculations are available for Δr ¹³⁸ and for the Z boson observables¹³⁹.

A possible mass splitting between \tilde{b}_L and \tilde{t}_L yields a contribution to the ρ -parameter of the same sign as the standard top term. As a universal loop contribution, it enters the quantity Δr and the Z boson couplings and is thus significantly constrained by the data on M_W and the leptonic widths. Recently the 2-loop α_s corrections have been computed¹⁴⁰, which can amount to 30% of the 1-loop $\Delta\rho_{\tilde{b}\tilde{t}}$.

Figure 14 displays the range of predictions for M_W in the minimal model and in the MSSM. It is thereby assumed that no direct discovery has been made at LEP 2. As can be seen, precise determinations of M_W and m_t can become decisive for the separation between the models.

As the standard model, the MSSM yields a good de-

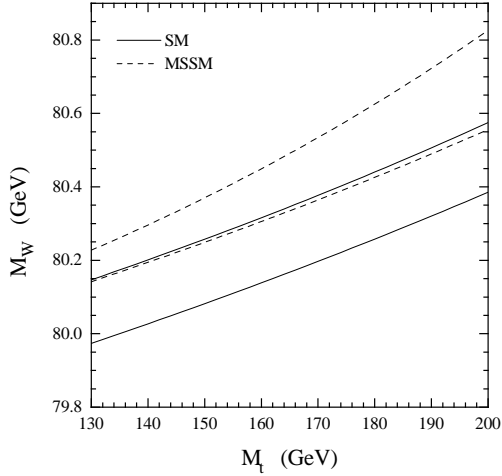


Figure 14: The W mass range in the standard model (—) and the MSSM (---). Bounds are from the non-observation of Higgs bosons and SUSY particles at LEP2.

scription of the precision data. A global fit⁹² to all electroweak precision data, including the top mass measurement, shows that the χ^2 of the fit is slightly better than in the standard model; but, owing to the larger numbers of parameters, the probability is about the same as for the standard model (Figure 15).

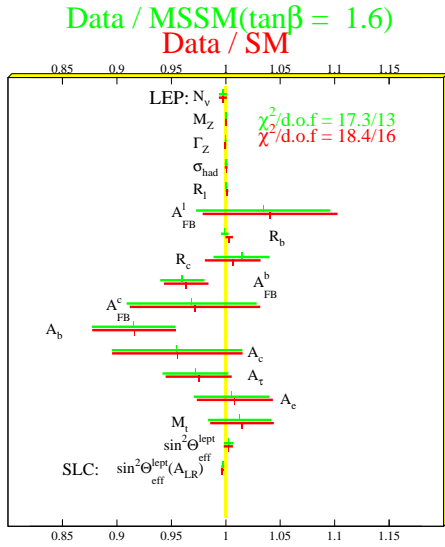


Figure 15: Best fits in the SM and in the MSSM, normalized to the data. Error bars are those from data. (Updated from ref⁹².)

The virtual presence of SUSY particles in the precision observables can be exploited also in the other way of constraining the allowed range of the MSSM parameters. Since the quality of the standard model description can be achieved only for those parameter sets where the standard model with a light Higgs boson is approximated,

deviations from this scenario result in a rapid decrease of the fit quality. An analysis of the precision data in this spirit can be found in ref¹⁴¹.

8 Conclusions

The experimental data for tests of the standard model have achieved an impressive accuracy. In the meantime, many theoretical contributions have become available to improve and stabilize the standard model predictions and to reach a theoretical accuracy clearly better than 0.1%.

The overall agreement between theory and experiment for the entire set of the precision observables is remarkable and instructively confirms the validity of the standard model. Fluctuations of data around the predictions are within two standard deviations, with no compelling evidence for deviations. Direct and indirect determinations of the top mass are compatible, and a light Higgs boson is clearly favoured by the analysis of precision data in the standard model context, which is far below the mass range where the standard Higgs sector becomes non-perturbative.

As a consequence of the high quality performance of the standard model, any kind of New Physics can only provoke small effects, at most of the size that is set by the radiative corrections. The MSSM, mainly theoretically advocated, is competitive to the standard model in describing the data with about the same quality in global fits. Since the MSSM predicts the existence of a light Higgs boson, the detection of a Higgs at LEP could be an indication of supersymmetry. The standard model can also accommodate such a light Higgs, but with the consequence that its validity cannot be extrapolated to energies much higher than the TeV scale.

Acknowledgements

I want to thank D. Bardin, G. Degrossi, A. Denner, S. Dittmaier, J. Erler, P. Gambino, F. Jegerlehner, J. Körner, J. Kühn, M. Neubert, G. Passarino, B. Ward, G. Weiglein for helpful discussions and support, W. de Boer and U. Schwickerath for updated fits in the MSSM, and A. Blondel, R. Clare, M. Grünwald, D. Karlen for providing me with valuable information on the experimental data.

References

1. The LEP Collaborations ALEPH, DELPHI, L3, OPAL, the LEP Electroweak Working Group and the SLD Heavy Flavor Working Group, CERN-PPE/97-154 (1997); M. Grünwald, talk at ICHEP98 (PS1), these proceedings

2. D. Karlen, plenary talk at ICHEP98, these proceedings
3. UA2 Collaboration, J. Alitti et al., *Phys. Lett. B* **276**, 354 (1992);
CDF Collaboration, F. Abe et al., *Phys. Rev. Lett.* **65**, 2243 (1990); *Phys. Rev. D* **43**, 2070 (1991); *Phys. Rev. Lett.* **75**, 11 (1995); *Phys. Rev. D* **52**, 4784 (1995);
D0 Collaboration, B. Abbott et al., *Phys. Rev. Lett.* **80**, 3008 (1998);
P. Derwent, A. Kotwal, talks at ICHEP98 (PS1), these proceedings
4. CDF Collaboration, F. Abe et al., *Phys. Rev. Lett.* **74**, 2626 (1995);
D0 Collaboration, S. Abachi et al., *Phys. Rev. Lett.* **74**, 2632 (1995)
5. R. Partridge, plenary talk at ICHEP98, these proceedings
6. G. 't Hooft, *Nucl. Phys. B* **33**, 173 (1971) and **35**, 167 (1971)
7. G. Passarino, M. Veltman, *Nucl. Phys. B* **160**, 151 (1979)
8. M. Consoli, *Nucl. Phys. B* **160**, 208 (1979)
9. A. Sirlin, *Phys. Rev. D* **22**, 971 (1980);
W. J. Marciano, A. Sirlin, *Phys. Rev. D* **22**, 2695 (1980);
A. Sirlin, W. J. Marciano, *Nucl. Phys. B* **189**, 442 (1981)
10. D.Yu. Bardin, P.Ch. Christova, O.M. Fedorenko, *Nucl. Phys. B* **175**, 435 (1980) and **197**, 1 (1982);
D.Yu. Bardin, M.S. Bilenky, G.V. Mithselmakher, T. Riemann, M. Sachwitz, *Z. Phys. C* **44**, 493 (1989)
11. J. Fleischer, F. Jegerlehner, *Phys. Rev. D* **23**, 2001 (1981)
12. K.I. Aoki, Z. Hioki, R. Kawabe, M. Konuma, T. Muta, *Suppl. Prog. Theor. Phys.* **73**,1 (1982);
Z. Hioki, *Phys. Rev. Lett.* **65**, 683 (1990), E: *ibidem* **65**, 1692 (1990); *Z. Phys. C* **49**, 287 (1991)
13. M. Consoli, S. LoPresti, L. Maiani, *Nucl. Phys. B* **223**, 474 (1983)
14. D.Yu. Bardin, M.S. Bilenky, G.V. Mithselmakher, T. Riemann, M. Sachwitz, *Z. Phys. C* **44**, 493 (1989)
15. M. Böhm, W. Hollik, H. Spiesberger, *Fortschr. Phys.* **34**, 687 (1986)
16. W. Hollik, *Fortschr. Phys.* **38**, 165 (1990)
17. M. Consoli, W. Hollik, F. Jegerlehner, in: *Z Physics at LEP 1*, eds. G. Altarelli, R. Kleiss and C. Verzegnassi, CERN 89-08 (1989)
18. G. Passarino, R. Pittau, *Phys. Lett. B* **228**, 89 (1989);
V.A. Novikov, L.B. Okun, M.I. Vysotsky, *Nucl. Phys. B* **397**, 35 (1993)
19. G. Passarino, M. Veltman, *Phys. Lett. B* **237**, 537 (1990)
20. W.J. Marciano, A. Sirlin, *Phys. Rev. Lett.* **46**, 163 (1981);
A. Sirlin, *Phys. Lett. B* **232**, 123 (1989)
21. G. Degrassi, S. Fanchiotti, A. Sirlin, *Nucl. Phys. B* **351**, 49 (1991)
22. G. Degrassi, A. Sirlin, *Nucl. Phys. B* **352**, 342 (1991)
23. M. Veltman, *Phys. Lett. B* **91**, 95 (1980);
M. Green, M. Veltman, *Nucl. Phys. B* **169**, 137 (1980), E: *Nucl. Phys. B* **175**, 547 (1980);
F. Antonelli, M. Consoli, G. Corbo, *Phys. Lett. B* **91**, 90 (1980);
F. Antonelli, M. Consoli, G. Corbo, O. Pellegrino, *Nucl. Phys. B* **183**, 195 (1981)
24. D.C. Kennedy, B.W. Lynn, *Nucl. Phys. B* **322**, 1 (1989)
25. M. Kuroda, G. Moulataka, D. Schildknecht, *Nucl. Phys. B* **350**, 25 (1991)
26. *Reports of the Working Group on Precision Calculations for the Z Resonance*, CERN 95-03 (1995), eds. D. Bardin, W. Hollik, G. Passarino
27. G. Källén, A. Sabry, *K. Dan. Vidensk. Selsk. Mat.-Fys. Medd.* **29** (1955) No. 17
28. M. Steinhauser, *Phys. Lett. B* **429**, 158 (1998)
29. S. Eidelman, F. Jegerlehner, *Z. Phys. C* **67**, 585 (1995)
30. H. Burkhardt, B. Pietrzyk, *Phys. Lett. B* **356**, 398 (1995)
31. M.L. Swartz, *Phys. Rev. D* **53**, 5268 (1996)
32. R. Alemany, M. Davier, A. Höcker, *Eur. Phys. J. C* **2** (1998) 123
33. M. Davier, A. Höcker, *Phys. Lett. B* **419**, 419 (1998); hep-ph/9801361; hep-ph/9805470
34. A. Höcker, talk at ICHEP98 (PS1), these proceedings
35. J.H. Kühn, M. Steinhauser, hep-ph/9802241
36. S. Groote, J. Körner, K. Schilcher, N.F. Nasrallah, hep-ph/9802374
37. J. Erler, hep-ph/9803453
38. A.H. Hoang, J.H. Kühn, T. Teubner, *Nucl. Phys. B* **452**, 173 (1995);
K.G. Chetyrkin, J.H. Kühn, M. Steinhauser, *Phys. Lett. B* **371**, 93 (1996); *Nucl. Phys. B* **482**, 213 (1996); **505**, 40 (1997);
K.G. Chetyrkin, R. Harlander, J.H. Kühn, M. Steinhauser, *Nucl. Phys. B* **503**, 339 (1997)
39. A.D. Martin, D. Zeppenfeld, *Phys. Lett. B* **345**, 558 (1995)
40. E. Braaten, S. Narison, A. Pich, *Nucl. Phys. B* **373** (1992) 581
41. Z. Zhan, talk at ICHEP98 (PS1), these proceedings

42. F. Jegerlehner, IVth International Symposium on Radiative Corrections, Barcelona, September 1998 (to appear in the proceedings, ed. J. Solà); F. Jegerlehner, O.V. Tarasov, hep-ph/9809485
43. D. Ross, M. Veltman, *Nucl. Phys. B* **95**, 135 (1975)
44. M. Veltman, *Nucl. Phys. B* **123**, 89 (1977); M.S. Chanowitz, M.A. Furman, I. Hinchliffe, *Phys. Lett. B* **78**, 285 (1978)
45. J.J. van der Bij, F. Hoogeveen, *Nucl. Phys. B* **283**, 477 (1987)
46. R. Barbieri, M. Beccaria, P. Ciafaloni, G. Curci, A. Vicere, *Phys. Lett. B* **288**, 95 (1992); *Nucl. Phys. B* **409**, 105 (1993); J. Fleischer, F. Jegerlehner, O.V. Tarasov, *Phys. Lett. B* **319**, 249 (1993)
47. A. Djouadi, C. Verzegnassi, *Phys. Lett. B* **195**, 265 (1987)
48. L. Avdeev, J. Fleischer, S. M. Mikhailov, O. Tarasov, *Phys. Lett. B* **336**, 560 (1994); E: *Phys. Lett. B* **349**, 597 (1995); K.G. Chetyrkin, J.H. Kühn, M. Steinhauser, *Phys. Lett. B* **351**, 331 (1995)
49. M. Veltman, *Acta Phys. Polon. B* **8**, 475 (1977)
50. J.J. van der Bij, M. Veltman, *Nucl. Phys. B* **231**, 205 (1985)
51. R.E. Behrends, R.J. Finkelstein, A. Sirlin, *Phys. Rev.* **101**, 866 (1956); T. Kinoshita, A. Sirlin, *Phys. Rev.* **113**, 1652 (1959)
52. T. van Ritbergen, R. Stuart, hep-ph/9802341; hep-ph/9808283
53. Particle Data Group, C. Caso et al., *Eur. Phys. J. C* **3**, 1 (1998)
54. J.H. Kühn, talk at ICHEP98 (PS1), these proceedings
55. W.J. Marciano, *Phys. Rev. D* **20**, 274 (1979)
56. M. Consoli, W. Hollik, F. Jegerlehner, *Phys. Lett. B* **227**, 167 (1989)
57. A. Djouadi, *Nuovo Cim. A* **100**, 357 (1988); D. Yu. Bardin, A.V. Chizhov, Dubna preprint E2-89-525 (1989); B.A. Kniehl, *Nucl. Phys. B* **347**, 86 (1990); F. Halzen, B.A. Kniehl, *Nucl. Phys. B* **353**, 567 (1991) 567; A. Djouadi, P. Gambino, *Phys. Rev. D* **49**, 3499 (1994)
58. B.A. Kniehl, J.H. Kühn, R.G. Stuart, *Phys. Lett. B* **214**, 621 (1988); B.A. Kniehl, A. Sirlin, *Nucl. Phys. B* **371**, 141 (1992); *Phys. Rev. D* **47**, 883 (1993); S. Fanchiotti, B.A. Kniehl, A. Sirlin, *Phys. Rev. D* **48**, 307 (1993)
59. K. Chetyrkin, J.H. Kühn, M. Steinhauser, *Phys. Rev. Lett.* **75**, 3394 (1995)
60. A. Sirlin, *Phys. Rev. D* **29**, 89 (1984)
61. G. Degrassi, P. Gambino, A. Vicini, *Phys. Lett. B* **383**, 219 (1996); G. Degrassi, P. Gambino, A. Sirlin, *Phys. Lett. B* **394**, 188 (1997); G. Degrassi, P. Gambino, M. Passera, A. Sirlin, *Phys. Lett. B* **418**, 209 (1998)
62. S. Bauberger, G. Weiglein, *Nucl. Instrum. Meth. A* **389**, 318 (1997); *Phys. Lett. B* **419**, 333 (1997)
63. G. Weiglein, *Acta Phys. Polon. B* **29**, 2735 (1998)
64. W. Hollik, B. Krause, A. Strempl, G. Weiglein, to appear; A. Strempl, Diploma Thesis (Karlsruhe 1998)
65. D. Bardin et al., *Reports of the Working Group on Precision Calculations for the Z Resonance*, p. 7, CERN 95-03 (1995), eds. D. Bardin, W. Hollik, G. Passarino; hep-ph/9709229
66. G. Degrassi, P. Gambino, A. Sirlin, TUM-HEP-333/98 (to appear), and private communication
67. A.A. Akhundov, D.Yu. Bardin, T. Riemann, *Nucl. Phys. B* **276**, 1 (1986); W. Beenakker, W. Hollik, *Z. Phys. C* **40**, 141 (1988); J. Bernabeu, A. Pich, A. Santamaria, *Phys. Lett. B* **200**, 569 (1988)
68. A. Denner, W. Hollik, B. Lampe, *Z. Phys. C* **60**, 193 (1993)
69. K.G. Chetyrkin, A.L. Kataev, F.V. Tkachov, *Phys. Lett. B* **85**, 277 (1979); M. Dine, J. Sapirstein, *Phys. Rev. Lett.* **43**, 668 (1979); W. Celmaster, R. Gonsalves, *Phys. Rev. Lett.* **44**, 560 (1980); S.G. Gorishny, A.L. Kataev, S.A. Larin, *Phys. Lett. B* **259**, 144 (1991); L.R. Surguladze, M.A. Samuel, *Phys. Rev. Lett.* **66**, 560 (1991); A. Kataev, *Phys. Lett. B* **287**, 209 (1992)
70. K.G. Chetyrkin, J.H. Kühn, *Phys. Lett. B* **248**, 359 (1990) and B **406**, 102 (1997); K.G. Chetyrkin, J.H. Kühn, A. Kwiatkowski, *Phys. Lett. B* **282**, 221 (1992); K.G. Chetyrkin, A. Kwiatkowski, *Phys. Lett. B* **305**, 285 (1993) and B **319**, 307 (1993)
71. B.A. Kniehl, J.H. Kühn, *Phys. Lett. B* **224**, 229 (1990); *Nucl. Phys. B* **329**, 547 (1990); K.G. Chetyrkin, J.H. Kühn, *Phys. Lett. B* **307**, 127 (1993); S. Larin, T. van Ritbergen, J.A.M. Vermaseren, *Phys. Lett. B* **320**, 159 (1994); K.G. Chetyrkin, O.V. Tarasov, *Phys. Lett. B* **327**, 114 (1994)
72. K.G. Chetyrkin, J.H. Kühn, A. Kwiatkowski, in

- Reports of the Working Group on Precision Calculations for the Z Resonance*, p. 175, CERN 95-03 (1995), eds. D. Bardin, W. Hollik, G. Passarino; K.G. Chetyrkin, J.H. Kühn, A. Kwiatkowski, *Phys. Rep.* **277**, 189 (1996)
73. J. Fleischer, F. Jegerlehner, P. Rączka, O.V. Tarasov, *Phys. Lett. B* **293**, 437 (1992); G. Buchalla, A.J. Buras, *Nucl. Phys. B* **398**, 285 (1993); G. Degrossi, *Nucl. Phys. B* **407**, 271 (1993); K.G. Chetyrkin, A. Kwiatkowski, M. Steinhauser, *Mod. Phys. Lett. A* **8**, 2785 (1993)
74. A. Kwiatkowski, M. Steinhauser, *Phys. Lett. B* **344**, 359 (1995); S. Peris, A. Santamaria, *Nucl. Phys. B* **445**, 252 (1995)
75. R. Harlander, T. Seidensticker, M. Steinhauser, *Phys. Lett. B* **426**, 125 (1998)
76. A. Czarnecki, J.H. Kühn, *Phys. Rev. Lett.* **77**, 3955 (1996); *E*: **80**, 893 (1998)
77. A. Hoang, J.H. Kühn, T. Teubner, *Nucl. Phys. B* **455**, 3 (1995); **452**, 173 (1995)
78. F.A. Berends et al., in: *Z Physics at LEP 1*, CERN 89-08 (1989), eds. G. Altarelli, R. Kleiss, C. Verzegnassi, Vol. I, p. 89; W. Beenakker, F.A. Berends, S.C. van der Marck, *Z. Phys. C* **46**, 687 (1990); G. Burgers, F.A. Berends, W.L. van Neerven, *Nucl. Phys. B* **297**, 429 (1988); *E*: **304**, 921 (1988); W. Beenakker, F.A. Berends, S.C. van der Marck, *Z. Phys. C* **46**, 687 (1990)
79. S. Jadach, M. Skrzypek, B.F.L. Ward, *Phys. Lett. B* **257**, 173 (1991); S. Jadach, M. Skrzypek, *Z. Phys. C* **49**, 584 (1991); G. Montagna, O. Nicosini, F. Piccinini, *Phys. Lett. B* **406**, 243 (1997)
80. S. Jadach et al., in *Reports of the Working Group on Precision Calculations for the Z Resonance*, CERN 95-03 (1995), p. 341, eds. D. Bardin, W. Hollik, G. Passarino; S. Jadach, O. Nicosini, in *Physics at LEP 2*, CERN 96-01, Vol. 1, eds. G. Altarelli, T. Sjöstrand, F. Zwirner
81. B.F.L. Ward, talk at ICHEP98 (PS1), these proceedings; B.F.L. Ward, S. Jadach, M. Melles, S.A. Yost, hep-ph/9811245
82. SLD Collaboration, S. Fahey, talk at ICHEP98 (PS1), these proceedings
83. P. Gambino, A. Sirlin, *Phys. Rev. Lett.* **73**, 621 (1994)
84. Yu. Dokshitzer, plenary talk at ICHEP98, these proceedings
85. G.L. Fogli, D. Haidt, *Z. Phys. C* **40**, 379 (1988); CDHS Collaboration, H. Abramowicz et al., *Phys. Rev. Lett.* **57**, 298 (1986); A. Blondel et al., *Z. Phys. C* **45**, 361 (1990); CHARM Collaboration, J.V. Allaby et al., *Phys. Lett. B* **177**, 446 (1987); *Z. Phys. C* **36**, 611 (1987); CHARM II Collaboration, D. Geiregat et al., *Phys. Lett. B* **247**, 131 (1990) and **259**, 499 (1991); CCFR Collaboration, C.G. Arroyo et al., *Phys. Rev. Lett.* **72**, 3452 (1994); *Eur. Phys. J. C* **1**, 509 (1998)
86. NuTeV Collaboration, T. Bolton, talk at ICHEP98 (PS1), these proceedings
87. D. Bardin et al., hep-ph/9412201
88. G. Montagna, O. Nicosini, F. Piccinini, G. Passarino, hep-ph/9804211
89. D. Bardin, G. Passarino, hep-ph/9803425
90. J. Erler, P. Langacker, hep-ph/9809352; hep-ph/9801422
91. K. Hagiwara, D. Haidt, S. Matsumoto, *Eur. Phys. J. C* **2**, 95 (1998); J. Ellis, G.L. Fogli, E. Lisi, *Phys. Lett. B* **389**, 321 (1996); *Z. Phys. C* **69**, 627 (1996); G. Passarino, *Acta Phys. Polon.* **28**, 635 (1997); S. Dittmaier, D. Schildknecht, *Phys. Lett. B* **391**, 420 (1997); S. Dittmaier, D. Schildknecht, G. Weiglein, *Phys. Lett. B* **386**, 247 (1996); P. Chankowski, S. Pokorski, *Acta Phys. Polon.* **27**, 1719 (1996)
92. W. de Boer, A. Dabelstein, W. Hollik, W. Mösle, U. Schwickerath, *Z. Phys. C* **75**, 627 (1997)
93. Z. Kunszt et al., in *Physics at LEP 2*, CERN 96-01, Vol. 1, p. 141, eds. G. Altarelli, T. Sjöstrand, F. Zwirner
94. W. Beenakker et al., in *Physics at LEP 2*, CERN 96-01, Vol. 1, p. 79, eds. G. Altarelli, T. Sjöstrand, F. Zwirner
95. S. Jadach et al., *Phys. Lett. B* **417**, 326 (1998); S. Jadach et al, contributed paper to ICHEP98, abstract 823 (PS1)
96. E.N. Argyres et al., *Phys. Lett. B* **358**, 339 (1995); U. Baur, D. Zeppenfeld, *Phys. Rev. Lett.* **75**, 1002 (1995); C. Papadopoulos, *Phys. Lett. B* **352**, 144 (1995)
97. G. Lopez Castro, J.L. Lucio M., J. Pestieau, *Int. J. Mod. Phys. A* **11**, 563 (1996); M. Beuthe, R. Gonzalez Felipe, G. Lopez Castro, J. Pestieau, *Nucl. Phys. B* **498**, 55 (1997)
98. W. Beenakker et al., *Nucl. Phys. B* **500**, 255 (1997)
99. W. Beenakker, A. Denner, *Acta Phys. Polon.* **B 29**, 2821 (1998)
100. W. Beenakker, A.P. Chapovsky, F.A. Berends, *Nucl. Phys. B* **508**, 17 (1997); *Phys. Lett. B*

- 411, 203 (1997)
101. A. Denner, S. Dittmaier, S. Roth, *Nucl. Phys. B* **519**, 39 (1998); *Phys. Lett. B* **429**, 145 (1998).
The original results of the earlier calculation
K. Melnikov, O. Yakovlev, *Nucl. Phys. B* **471**, 90 (1996)
does not agree with the other two more recent results. As known from the authors, their corrected result is now also in agreement (O. Yakovlev, private communication; and Erratum, to appear)
102. V.S. Fadin, V.A. Khoze, A.D. Martin, *Phys. Rev. D* **49**, 2247 (1994);
K. Melnikov, O. Yakovlev, *Phys. Lett. B* **324**, 217 (1994)
103. U. Baur, talk at ICHEP98 (PS1), these proceedings;
U. Baur, S. Keller, D. Wackerroth, hep-ph/9807417
104. D. Wackerroth, W. Hollik, *Phys. Rev. D* **55**, 6788 (1997)
105. M. Passera, A. Sirlin, *Acta Phys. Polon. B* **29** 2901 (1998)
106. D. Treille, plenary talk at ICHEP98, these proceedings
107. L. Maiani, G. Parisi, R. Petronzio, *Nucl. Phys. B* **136**, 115 (1979);
N. Cabibbo, L. Maiani, G. Parisi, R. Petronzio, *Nucl. Phys. B* **158**, 259 (1979);
R. Dashen, H. Neuberger, *Phys. Rev. Lett.* **50**, 1897 (1983);
D.J.E. Callaway, *Nucl. Phys. B* **233**, 189;
M.A. Beg, C. Panagiotakopoulos, A. Sirlin, *Phys. Rev. Lett.* **52**, 883 (1984);
M. Lindner, *Z. Phys. C* **31**, 295 (1986)
108. M. Lindner, M. Sher, H. Zaglauer, *Phys. Lett. B* **228**, 139 (1989);
G. Altarelli, G. Isidori, *Phys. Lett. B* **337**, 141 (1994);
J.A. Casas, J.R. Espinosa, M. Quiros, *Phys. Lett. B* **342**, 171 (1995) and **382**, 374 (1996);
109. T. Hambye, K. Riesselmann, *Phys. Rev. D* **55**, 7255 (1997)
110. Kuti et al., *Phys. Rev. Lett.* **61**, 678 (1988);
P. Hasenfratz et al., *Nucl. Phys. B* **317**, 81 (1989);
M. Lüscher, P. Weisz, *Nucl. Phys. B* **318**, 705 (1989);
M. Göckeler, H. Kastrup, T. Neuhaus, F. Zimmermann, *Nucl. Phys. B* **404**, 517 (1993)
111. M. Göckeler, H. Kastrup, J. Westphalen, F. Zimmermann, *Nucl. Phys. B* **425**, 413 (1994)
112. A. Ghinculov, *Nucl. Phys. B* **455**, 21 (1995);
A. Frink, B. Kniehl, K. Riesselmann, *Phys. Rev. D* **54**, 4548 (1996)
113. T. Binoth, A. Ghinculov, J.J. van der Bij, *Phys. Rev. D* **57**, 1487 (1998); *Phys. Lett. B* **417**, 343 (1998)
114. L. Durand, B.A. Kniehl, K. Riesselmann, *Phys. Rev. Lett.* **72**, 2534 (1994); E: *ibidem B* **74**, 1699 (1995);
A. Ghinculov, *Phys. Lett. B* **337**, 137 (1994); E: *ibidem B* **346**, 426 (1995);
V. Borodulin, G. Jikia, *Phys. Lett. B* **391**, 434 (1997)
115. K. Riesselmann, hep-ph/9711456
116. K. Adel and Y.P. Yao, *Phys. Rev. D* **49**, 4945 (1994);
C. Greub and T. Hurth, *Phys. Rev. D* **56**, 2934 (1997);
A.J. Buras, A. Kwiatkowski and N. Pott, *Phys. Lett. B* **414**, 157 (1997); *Nucl. Phys. B* **517**, 353 (1998);
A. Ali and C. Greub, *Phys. Lett. B* **361**, 146 (1995);
C. Greub, T. Hurth and D. Wyler, *Phys. Lett. B* **380**, 385 (1996); *Phys. Rev. D* **54**, 3350 (1996);
K. Chetyrkin, M. Misiak and M. Münz, *Phys. Lett. B* **400**, 206 (1997); E: **425**, 414 (1998)
117. A. Czarnecki and W.J. Marciano, *Phys. Rev. Lett.* **81**, 277 (1998);
A.L. Kagan and M. Neubert, hep-ph/9805303
118. M. Neubert, talk at ICHEP98 (PS7), these proceedings; hep-ph/9809377
119. T. Skwarnicki (CLEO Collaboration), talk at ICHEP98 (PS7), these proceedings
120. R. Barate et al. (ALEPH Collaboration), *Phys. Lett. B* **429**, 169 (1998)
121. J. Hewett, M. Neubert, talks at ICHEP98 (PS16), these proceedings
122. V.W. Hughes, in: *Frontiers of High Energy Spin Physics*, Universal Academy Press, Tokyo 1992, p. 717, ed. T. Hasegawa
123. K. Fujikawa, B.W. Lee, A.I. Sanda, *Phys. Rev. D* **6**, 2923 (1972);
R. Jackiw, S. Weinberg, *Phys. Rev. D* **5**, 2473 (1972);
G. Altarelli, N. Cabibbo, L. Maiani, *Phys. Lett. B* **40**, 415 (1972);
I. Bars, M. Yoshimura, *Phys. Rev. D* **6**, 374 (1972);
W. Bardeen, R. Gastmans, B. Lautrup, *Nucl. Phys. B* **46**, 315 (1972)
124. S. Peris, M. Perrottet, E. de Rafael, *Phys. Lett. B* **355**, 523 (1995)
125. A. Czarnecki, B. Krause, W. Marciano, *Phys. Rev. D* **52**, 2619 (1995); *Phys. Rev. Lett.* **76**, 3267 (1996)
126. G. Degrassi, G.F. Giudice, hep-ph/9803384
127. K. Adel, F.J. Yndurain, hep-ph/9509378;
D.H. Brown, W.A. Worstell, *Phys. Rev. D* **54**, 3237 (1996)
128. M. Hayakawa, T. Kinoshita, A.I. Sanda, *Phys.*

- Rev. Lett.* **75**, 790 (1995); *Phys. Rev. D* **54**, 3137 (1996)
129. M. Hayakawa, T. Kinoshita, *Phys. Rev. D* **57**, 7267 (1997)
130. J. Bijnens, E. Pallante, J. Prades, *Nucl. Phys. B* **474**, 379 (1996); *Phys. Rev. Lett.* **75**, 1447 (1995); E: *ibidem* **75**, 3781 (1995)
131. B. Krause, *Phys. Lett. B* **390**, 392 (1997); T. Kinoshita, B. Nizic, Y. Okamoto, *Phys. Rev. D* **31**, 2108 (1985); T. Kinoshita, W. Marciano, in: *Quantum Electrodynamics*, ed. T. Kinoshita, World Scientific 1990 (p. 419)
132. T. Kinoshita, *Phys. Rev. Lett.* **75**, 4728 (1995); S. Laporta, E. Remiddi, *Phys. Lett. B* **379**, 283 (1996)
133. B. Krause, A. Czarnecki, *Phys. Rev. Lett.* **78**, 4339 (1997)
134. Y. Fukuda et al., hep-ex/9805006; hep-ex/9805021; hep-ex/987003; M. Takita, plenary talk at ICHEP98, these proceedings
135. M. Carena, J. Espinosa, M. Quiros, C. Wagner, *Phys. Lett. B* **355**, 209 (1995); M. Carena, M. Quiros, C. Wagner, *Nucl. Phys. B* **461**, 407 (1996); H. Haber, R. Hempfling, A. Hoang, *Z. Phys. C* **75**, 539 (1997); S. Heinemeyer, W. Hollik, G. Weiglein, *Phys. Rev. D* **58**, 091701 (1998); hep-ph/9807423 (*Phys. Lett. B*, to appear)
136. A. Denner, R. Guth, W. Hollik, J.H. Kühn, *Z. Phys. C* **51**, 695 (1991); J. Rosiek, *Phys. Lett. B* **252**, 135 (1990); M. Boulware, D. Finnell, *Phys. Rev. D* **44**, 2054 (1991)
137. G. Altarelli, R. Barbieri, F. Caravaglios, *Phys. Lett. B* **314**, 357 (1993); C.S. Lee, B.Q. Hu, J.H. Yang, Z.Y. Fang, *J. Phys. G* **19**, 13 (1993); Q. Hu, J.M. Yang, C.S. Li, *Commun. Theor. Phys.* **20**, 213 (1993); J.D. Wells, C. Kolda, G.L. Kane, *Phys. Lett. B* **338**, 219 (1994); G.L. Kane, R.G. Stuart, J.D. Wells, *Phys. Lett. B* **354**, 350 (1995); M. Drees et al., *Phys. Rev. D* **54**, 5598 (1996)
138. P. Chankowski, A. Dabelstein, W. Hollik, W. Mösle, S. Pokorski, J. Rosiek, *Nucl. Phys. B* **417**, 101 (1994); D. Garcia, J. Solà, *Mod. Phys. Lett. A* **9**, 211 (1994)
139. D. Garcia, R. Jiménez, J. Solà, *Phys. Lett. B* **347**, 309 and 321 (1995); D. Garcia, J. Solà, *Phys. Lett. B* **357**, 349 (1995); A. Dabelstein, W. Hollik, W. Mösle, in *Perspectives for Electroweak Interactions in e^+e^- Collisions*, Ringberg Castle 1995, ed. B.A. Kniehl, World Scientific 1995 (p. 345); P. Chankowski, S. Pokorski, *Nucl. Phys. B* **475**, 3 (1996); J. Bagger, K. Matchev, D. Pierce, R. Zhang, *Nucl. Phys. B* **491**, 3 (1997)
140. A. Djouadi, P. Gambino, S. Heinemeyer, W. Hollik, C. Jünger, G. Weiglein, *Phys. Rev. Lett.* **78**, 3626 (1997); *Phys. Rev. D* **57**, 4179 (1998)
141. J. Erler, D. Pierce, *Nucl. Phys. B* **526**, 53 (1998)

